TABLE OF CONTENTS

TABLE OF CONTENTS (cont'd)

THE QUANTUM CORRECTIONS TO THE TRANSPORT COLLISION INTEGRALS *

by

Herbert T. Wood +

University of Wisconsin Theoretical Chemistry Institute
Madison, Wisconsin

ABSTRACT

The second quantum correction to the phase shift in a collision between particles with spherically symmetric potentials is obtained, using the method of Curtiss and Powers. In this expression the potential is not restricted to monotonic functions; the results apply to a potential with an attractive minimum. The classical limit and the first quantum correction, both developed earlier for monotonic potentials, are also rederived so that they may be used with potentials possessing a minimum. These expressions are then used to develop series expressions for $Q^{(1)}$ and $Q^{(2)}$, the so-called cross sections for diffusion and viscosity, respectively. These expressions for $Q^{(1)}$ and $Q^{(2)}$ are used to obtain the classical limit and the quantum corrections to the transport collision integrals.

In the case of $Q^{(2)}$ the effect of statistics on collisions between like molecules is also considered. It is found that $Q^{(2)}$ is not modified by statistics, at least through terms of order $\hbar^4$.

- - - - -

* This research was supported by the following grant:
National Aeronautics and Space Administration Grant NsG-275-62.

+ National Science Foundation Fellow 1963-1965.

ACKNOWLEDGEMENTS

This is the best opportunity I know of to express my sincere thanks to my Major Professor, Dr. Charles F. Curtiss, because without his help this thesis could never have been started, developed, or completed. His even disposition and immense reservoir of patience (which was severely drained at times during the period of this work) will always remain as a source of amazement to me.

Encouragement and interest from Professor J. O. Hirschfelder was very helpful. Professor Richard B. Bernstein's interest and enthusiasm during the course of this work was also appreciated. Here it seems only fitting to thank Professors Frank Andrews and Paul Bender in addition to the above for taking the time to write a multitudinous number of reference reports for me.

Doubly thanked are Mrs. Mary Wilson, Mrs. Margie Heil, and Mr. Thomas Mann. It was only through their tireless effort of many late hours that this thesis was typed and reproduced. Such devotion to job is difficult to find.

My thanks are also extended to my fellow students at the ICI, the computing staff, NASA, and the National Science Foundation. In countless ways these groups have made my stay here at Wisconsin very enjoyable and stimulating.

Needless to say, I would also like to extend thanks to my little family, Kathy, Kevin and Amy, who could always be counted on to provide the periodic cheering up every graduate student needs. Even when he's finishing up.

LIST OF FIGURES

LIST OF TABLES

CHAPTER I

INTRODUCTION

At the macroscopic level the interaction of objects is an easily observed phenomenon. From such observations it is possible, using Newtonian mechanics, to calculate changes that occur in a system as a result of the interaction. In particular, the transport of mass, momentum and energy from one part of the system to another can be calculated. It is possible to do this for two reasons: (1) the objects are large enough to be seen, and (2) a finite time is required for the process to occur. This can be demonstrated by considering a batter disturbing the steady state of a baseball in flight from the pitcher to the catcher by hitting it. The bat imparts momentum and energy to the ball and changes the position of its mass from home plate to the outfield. These three quantities are transferred to an outfielder (if he can catch the ball on the fly). By observing the flight of the ball one could calculate the amount of mass, momentum, and energy transferred.

At the molecular level we are denied one of the two advantages given above. In the study of molecular phenomena we are blind. However, because it does take a finite time for the mass, momentum, and energy to be distributed throughout the system, it is possible to observe the effect of these transfers. We call the properties of the gas which represent the rate at which these transport processes take place, the diffusion coefficient, viscosity, and thermal

conductivity respectively.

The mechanism by which these transport processes take place is molecular motion and collisions. It is the purpose of the kinetic theory of gases to relate these macroscopic properties to the interaction of the particles on a molecular level. Thus, one must understand the dynamics of the collision process.

The development[1] of the kinetic theory began with the pioneering work of Clausius, Maxwell, and Boltzmann in the last half of the nineteenth century. It reached its first plateau of development with the publication by Boltzmann[2] of his paper on the integro-differential equation for the time development of the distribution function which describes the state of the gas. In developing this equation Boltzmann considered collisions that involved two particles. He was limited to collisions of this low order because of the complexity of the mathematics involved in treating collisions of more than two particles. In studying these collisions he used the tools at hand, Newtonian mechanics. His integro-differential equation proved to be so intractable that it defied solution for forty-four years.

The solution of Boltzmann's equation was the second plateau in the development of the kinetic theory of gases. This feat was accomplished almost simultaneously by Chapman[3] in England and Enskog[4] in Sweden. They arrived at integral expressions for the transport coefficients which involved the parameters of a collision: the angle of deflection, the impact parameter, and the energy of a

collision. They also introduced into the equations the important fundamental concept of a cross section for a collision. It is this quantity which serves as a link between the classical and quantum treatment.

After the discovery of quantum mechanics in 1925, it was recognized that Boltzmann's treatment was an approximation in that he had treated the collisions classically. It became necessary, therefore, to modify Boltzmann's work to treat the collisions quantum mechanically.

The treatment of scattering theory using quantum mechanics proved to be much more difficult than the same problem treated classically. In the first place, the uncertainty principle makes the exact definition of such things as an angle of deflection and an impact parameter impossible. However, the concept of a cross section for a collision, which is the probability that a particle will be scattered in a given direction, is consistent with the quantum picture. With this premise Uhlenbeck and Uehling[5] in 1932 (and later Massey and Mohr[6]) recast Boltzmann's collision integral into a form containing the cross section. Classically the cross section is a function of the energy and the angle of deflection and has the form

$$\sigma(E,\chi) = \frac{b}{\sin\chi}\left|\frac{db}{d\chi}\right| \qquad (1\text{-}1)$$

where χ is the angle of deflection, b is the impact parameter, and E is the energy.

The corresponding expression in quantum mechanics was derived by Faxen and Holtsmark[7] in 1927. For collisions involving particles that are not alike (that are distinguishable) the cross section is

$$\sigma(E,\chi) = \frac{\hbar^2}{4E}\left|\sum_{l=0}^{\infty}(2l+1)(e^{2i\eta_l}-1)P_l(\cos\chi)\right| \quad (1\text{-}2)$$

where P_l is the l^{th} Legendre polynomial, η_l is the l^{th} phase shift (to be defined later) for the collision, and $\hbar$ is Planck's constant divided by 2π and the square root of twice the reduced mass of the colliding particles. In the event that the particles are identical the Pauli principle leads to a modification of this expression (the treatment of identical particles points out the second major difference between classical and quantum mechanics. In classical mechanics the particles, even identical particles, can be followed along their entire trajectories. In quantum mechanics the particles, if they are identical, can only be "observed" separately before the collision and then after the collision).

It is very easy, geometrically, to picture exactly the angle of deflection of a collision. The phase shift, while a little more difficult to picture conceptually, does have geometric significance. If we imagine that the collision takes place with one particle fixed and the other colliding with it (the one

dimensional reduced picture) we may represent the incoming particle as a plane wave. If the scatterer exerted no effect (the potential of interaction is zero) on the incoming wave, the wave would pass through the scattering center. For convenience, however, let us imagine the "scattered" wave as expanded in terms of spherical waves centered on the scatterer. Now let us suppose that the scatterer does exert some effect on the incoming wave. The exact nature of the effect will depend, of course, on the form of the intermolecular potential. Again we can expand the scattered (truly scattered this time) wave in terms of spherical waves. If we compare these two sets of waves at a point so far from the scattering center that its influence is nil, we would find that the spherical waves would not coincide. This is the result of the action of the scatterer. The difference, in radians, between the n^{th} zero (as counted from the scattering center) of the scattered wave and the n^{th} zero of the unscattered wave (both very far from the scattering center) for the same ℓ^{th} component of the spherical wave expansion is the phase shift η_ℓ (of course, the zero of the wave functions need not have been chosen; the n^{th} maximum, minimum, or any similar point on both waves could have been used.).

Once an expression for the cross section had been derived, it would seem to be straightforward to calculate the phase shifts and hence the transport properties. However, no exact formula for the phase shift exists, in general, and one is faced with the chore of fitting approximate methods into the scheme. Of course, one could

integrate Schrödinger's equation withand without the potential and get the phase shifts directly. Such a procedure has been used[8-12] and the transport properties calculated. This method suffers numerically in that for high energy the time required for the calculation is prohibitive. Thus, with this method one is restricted to low energy (the higher the energy, the greater the ℓ value necessary) and, thus, to low temperature. Another alternative is to use a semiclassical expression for the phase shift. This approach is effective at temperatures intermediate between the low temperature quantum range and the high temperature classical range. This procedure was first used by de Boer and Bird[13] in 1954. They used the phase shift series and found the first quantum correction to the transport properties for purely repulsive potentials. An analogous procedure, not restricted to repulsive potentials, is used in this thesis. The semiclassical method used is that due to Curtiss and Powers.[14]

In this thesis the Curtiss-Powers expression for the phase shift, which gives the phase shift as a series in powers of Planck's constant, is extended to three terms. Expressions for the first two moments of the cross section, $Q^{(1)}$ and $Q^{(2)}$ (the so-called cross section for diffusion and viscosity, respectively), are then derived as power series in $\hbar$ to the $\hbar^4$ term (for dimensional considerations the ordering parameter is changed from $\hbar$ to de Boer's dimensionless quantum parameter Λ^*). From these

expressions the omega integrals, $\Omega^{(1,1)}$ and $\Omega^{(2,2)}$ are obtained, again as a series in Λ^*.

CHAPTER II

THE QUANTUM CORRECTIONS AND THE TRANSPORT PROPERTIES

The second quantum correction to the phase shift in a collision between particles with spherically symmetric potentials is obtained, using the method of Curtiss and Powers.[14] In this expression the potential is not restricted to monotonic functions; the results apply to a potential with an attractive minimum. The classical limit and the first quantum correction, both developed earlier for monotonic potentials, are also rederived so that they may be used with potentials possessing a minimum. These expressions are then used to develop series expressions for $Q^{(1)}$ and $Q^{(2)}$, the so-called cross sections for diffusion and viscosity, respectively. For purely repulsive potentials this is a series in $\hbar^2$. For potentials with a minimum the series also contains terms in $\hbar$ and $\hbar^3$. These expressions for $Q^{(1)}$ and $Q^{(2)}$, in turn, are used to obtain the classical limit and the quantum corrections to the omega integrals $\Omega^{(1,1)}$ and $\Omega^{(2,2)}$. It is from these quantities that the transport properties are calculated.

In the case of $Q^{(2)}$ (and $\Omega^{(2,2)}$) the effect of statistics on collisions between like molecules is also considered. It is found that $Q^{(2)}$ (and thus $\Omega^{(2,2)}$) is not modified by statistics, at least through terms of order $\hbar^4$.

1. Quantum Corrections to the Transport Cross Sections for Repulsive Potentials.

The material contained in this section has been published previously.[15] A reprint of this publication forms Appendix I of this thesis. To preserve continuity, however, a brief resume of this paper is presented here.

In deriving the expressions for $Q^{(1)}$ and $Q^{(2)}$, it is necessary to start with the exact quantum mechanical form of $Q^{(1)}$ and $Q^{(2)}$. These are well known and were first derived in the form used in this work by Kramers. The higher moments of the cross section, $Q^{(3)}$, $Q^{(4)}$, etc., are needed for the higher approximations to the solution of Boltzmann's equation. The expression for $Q^{(3)}$ was apparently first published by Mason, Smith and Munn.[11] A general expression for $Q^{(l)}$ is derived in Appendix II.

Explicitly, the Kramers' expressions for $Q^{(1)}$ and $Q^{(2)}$ are

$$Q^{(1)} = \frac{4\pi}{E} \sum_{l=0}^{\infty} (l+1) \sin^2(\eta_{l+1} - \eta_l) \qquad (2.1\text{-}1)$$

$$Q^{(2)} = \frac{2\pi}{E} \sum_{l=0}^{\infty} \frac{(l+1)(l+2)}{(l+\frac{3}{2})} \sin^2(\eta_{l+2} - \eta_l) \qquad (2.1\text{-}2)$$

The Curtiss-Powers series for the phase shift is

$$\eta_l = \sum_{j=1}^{\infty} h^{2j-3} \eta_l^{(j)} \qquad (2.1\text{-}3)$$

Explicit expressions for $\eta_\ell^{(1)}$ and $\eta_\ell^{(2)}$ were obtained previously. The explicit expression for $\eta_\ell^{(3)}$ is

$$\eta_\ell^{(3)} = \int d\tau \, (E-\phi)^{-\frac{1}{2}} \times \tag{2.1-4}$$

$$\times \left[-\frac{5}{16\tau^5\phi'} - \frac{9\,\phi''}{64\tau^4\phi'^2} + \frac{\phi'''}{24\tau^3\phi'^2} - \frac{\phi''^2}{16\tau^3\phi'^3} \right.$$

$$- \frac{\phi^{(IV)}}{96\tau^2\phi'^2} + \frac{\phi''\phi'''}{24\tau^2\phi'^3} - \frac{\phi''^3}{32\tau^2\phi'^4} - \frac{\phi^{(VI)}}{576\,\phi'^2}$$

$$+ \frac{29\,\phi''\phi^{(V)}}{2880\,\phi'^3} + \frac{47\,\phi'''\phi^{(IV)}}{2880\,\phi'^3} - \frac{53\,\phi''^2\phi^{(IV)}}{1440\,\phi'^4}$$

$$\left. - \frac{7\,\phi''\phi'''^2}{144\,\phi'^4} + \frac{7\,\phi''^3\phi'''}{72\,\phi'^5} - \frac{7\,\phi''^5}{192\,\phi'^6} \right]$$

The Euler-Maclaurin approximation may be used to transform the sum over ℓ in $Q^{(1)}$ and $Q^{(2)}$ to an integral over ℓ plus correction terms. In addition, one transforms the integral over ℓ to an integration over L where L is defined as

$$L = (\ell + \tfrac{1}{2})h. \tag{2.1-5}$$

It is also convenient to define the following functions

$$\chi_{no} = n\frac{\partial \eta_\ell^{(1)}}{\partial L} \qquad \chi'_{no} = n\frac{\partial \chi_{no}}{\partial L} \qquad \chi''_{no} = n\frac{\partial \chi'_{no}}{\partial L}$$

$$\psi_{no} = n\frac{\partial \eta_\ell^{(2)}}{\partial L} \qquad \varphi_{no} = n\frac{\partial \eta_\ell^{(3)}}{\partial L} \tag{2.1-6}$$

Explicitly these functions are

$$\chi_{n0} = n\left[\frac{\pi}{2} - L\int d\tau\, \tau^{-2}(E-\phi)^{-\frac{1}{2}}\right] \tag{2.1-7}$$

$$\chi'_{n0} = -n\int d\tau\,(E-\phi)^{-\frac{1}{2}}\left[\frac{1}{\tau^2} + \frac{8L^2}{\tau^5\phi'} + \frac{2L^2\phi''}{\tau^4\phi'^2}\right] \tag{2.1-8}$$

$$\chi''_{n0} = -n\int d\tau\,(E-\phi)^{-\frac{1}{2}} \times \tag{2.1-9}$$

$$\times\left[\frac{24L}{\tau^5\phi'} + \frac{6L\phi''}{\tau^4\phi'^2} + \frac{168L^3}{\tau^8\phi'^2} + \frac{12L^3\phi''^2}{\tau^6\phi'^4} + \frac{72L^3\phi''}{\tau^7\phi'^3} - \frac{4L^3\phi'''}{\tau^6\phi'^3}\right]$$

$$\psi_{n0} = \frac{n}{12}L\int d\tau\,\tau^{-2}(E-\phi)^{-\frac{1}{2}} \times \tag{2.1-10}$$

$$\times\left[\frac{36}{\tau^3\phi'} + \frac{15\phi''}{\tau^2\phi'^2} + \frac{6\phi''^2}{\tau\,\phi'^3} - \frac{4\phi''\phi'''}{\phi'^3} + \frac{3\phi''^3}{\phi'^4} + \frac{\phi^{(iv)}}{\phi'^2}\right]$$

$$\varphi_{n0} = n \int d\tau \, (E - \phi)^{-\frac{1}{2}} \times \qquad (2.1\text{-}11)$$

$$\times \left[-\frac{469L}{16r^8\phi'^2} - \frac{353L\phi''}{16r^7\phi'^3} + \frac{523L\phi'''}{96r^6\phi'^3} - \frac{1169L\phi''^2}{96r^6\phi'^4} \right.$$
$$- \frac{71L\phi''^3}{12r^5\phi'^5} + \frac{6L\phi''\phi'''}{r^5\phi'^4} - \frac{31L\phi^{(iv)}}{30r^5\phi'^3} - \frac{5L\phi''^4}{2r^4\phi'^6}$$
$$- \frac{2L\phi'''^2}{3r^4\phi'^4} + \frac{193L\phi''^2\phi'''}{48r^4\phi'^5} - \frac{247L\phi''\phi^{(iv)}}{240r^4\phi'^4} + \frac{17L\phi^{(v)}}{120r^4\phi'^3}$$
$$- \frac{49L\phi''^5}{48r^3\phi'^7} + \frac{7L\phi''^3\phi'''}{3r^3\phi'^6} - \frac{35L\phi''\phi'''^2}{36r^3\phi'^5} - \frac{53L\phi''^2\phi^{(iv)}}{72r^3\phi'^5}$$
$$+ \frac{47L\phi'''\phi^{(iv)}}{180r^3\phi'^4} + \frac{29L\phi''\phi^{(v)}}{180r^3\phi'^4} - \frac{L\phi^{(vi)}}{48r^3\phi'^3} - \frac{49L\phi''^6}{96r^2\phi'^8}$$
$$+ \frac{49L\phi''^4\phi'''}{32r^2\phi'^7} - \frac{77L\phi''^2\phi'''^2}{72r^2\phi'^6} - \frac{9L\phi''^3\phi^{(iv)}}{16r^2\phi'^6} + \frac{37\phi''^2\phi^{(v)}}{240r^2\phi'^5}$$
$$+ \frac{17L\phi''\phi'''\phi^{(iv)}}{36r^2\phi'^5} - \frac{19L\phi'''\phi^{(v)}}{360r^2\phi'^4} - \frac{11L\phi''\phi^{(vi)}}{360r^2\phi'^4}$$
$$\left. - \frac{47L\phi^{(iv)2}}{1440r^2\phi'^4} + \frac{7L\phi'''^3}{72r^2\phi'^5} + \frac{L\phi^{(vii)}}{288r^2\phi'^3} \right]$$

where ϕ is the effective potential defined as

$$\phi = \varphi + \frac{L^2}{r^2} \qquad (2.1\text{-}12)$$

and φ is the intermolecular potential. The integration is carried out over the range of r such that

$$E - \phi > 0 \qquad (2.1\text{-}13)$$

In terms of these functions $Q^{(1)}$ and $Q^{(2)}$ are found to be

$$Q^{(1)} = \frac{4\pi}{E}\int_0^\infty L \sin^2 \chi_{10}\, dL \qquad (2.1\text{-}14)$$

$$+h^2 \frac{4\pi}{E}\left[\int_0^\infty dL\left[-\frac{1}{12}L(\chi'_{10})^2\cos 2\chi_{10} + \left(L\psi_{10} + \frac{1}{12}\chi'_{10}\right)\sin 2\chi_{10}\right] + \frac{1}{24}\right]$$

$$+h^4 \frac{4\pi}{E}\left[\int_0^\infty dL\left[\left[\frac{L}{360}(\chi''_{10})^2 + \frac{1}{6}L\chi''_{10}\psi_{10} + L\psi_{10}^2 + \frac{1}{720}L(\chi'_{10})^4 + \frac{1}{6}\chi'_{10}\psi_{10}\right]\cos 2\chi_{10} + \left[\frac{1}{360}(\chi'_{10})^3 + L\varphi_{10} - \frac{L}{6}(\chi'_{10})^2\psi_{10}\right]\sin 2\chi_{10}\right] - \frac{7}{960}(\chi'_{10}(0))^2\right]$$

$$Q^{(2)} = \frac{2\pi}{E}\int_0^\infty L \sin^2 \chi_{20}\, dL \qquad (2.1\text{-}15)$$

$$+h^2 \frac{2\pi}{E}\int_0^\infty dL\left[L\psi_{20}\sin 2\chi_{20} - \frac{1}{3}L(\chi'_{20})^2\cos 2\chi_{20} - \frac{1}{4L}\sin^2\chi_{20}\right]$$

$$+\hbar^4 \frac{2\pi}{E}\left[\int_0^\infty dL\left[\left[\left[\frac{2}{45}L(\chi_{20}'')^2+\frac{1}{45}L(\chi_{20}')^4+L\psi_{20}^2\right]\cos 2\chi_{20}\right.\right.\right.$$
$$\left.+\frac{2}{3}\chi_{20}'\psi_{20}+\frac{2}{3}L\chi_{20}''\psi_{20}\right]$$
$$+\left[\frac{2}{45}(\chi_{20}')^3-\frac{2}{3}L(\chi_{20}')^2\psi_{20}\right]\sin 2\chi_{20}$$
$$\left.\left.+L\psi_{20}-\frac{1}{24L}\chi_{20}''-\frac{1}{4L}\psi_{20}\right]\right]$$
$$\left.+\frac{119}{960}(\chi_{20}'(0))^2\right]$$

Since both $Q^{(1)}$ and $Q^{(2)}$ are expressed as power series in $\hbar^2$, these forms are useful in those cases where the quantum effects begin to play a small but significant role in collisions between molecules which interact through purely repulsive potentials.

2. Quantum Corrections to the Transport Cross Section for Potentials with a Minimum.

The existence of a minimum in the potential introduces two complications into the development of the cross sections as outlined in the previous section. The first of these difficulties arises in the derivation of the terms in the phase shift expansion, Eqn. (2.1-3). Since the effective potential has a maximum and a minimum for certain values of the energy and angular momentum, it is necessary in the derivation of $\eta_\ell^{(2)}$ and $\eta_\ell^{(3)}$ (but not $\eta_\ell^{(1)}$) to integrate by parts (see Eqn. (57) of reference 14) around these

points so that ϕ' does not appear in the denominator of the integrands (this point will be discussed in Chapter V.). This complication creates no great difficulty and the final expressions for $\eta_\ell^{(2)}$, $\eta_\ell^{(3)}$ and the functions derived from them (corresponding to those in Eqns. (2.1-8) through (2.1-11)) are

$$\eta_\ell^{(2)} = \frac{1}{24}\left[\int_{r_3, r_1, Q}^{\infty, V, r_2} dr\ (E-\phi)^{-\frac{1}{2}} \times \left[\frac{3}{r^2} - \frac{\phi'''}{\phi'} + \left(\frac{\phi''}{\phi'}\right)^2\right] + \frac{1}{2}\int_V^Q dr\left[(E-\phi)^{-\frac{3}{2}}\phi'' + (E-\phi)^{-\frac{1}{2}}\frac{6}{r^2}\right] + \frac{\phi''}{\phi'}(E-\phi)^{-\frac{1}{2}}\Big|_Q^V\right] \tag{2.2-1}$$

$$\eta_\ell^{(3)} = \int_{r_3, r_1, Q}^{\infty, V, r_2} dr\ (E-\phi)^{-\frac{1}{2}} \times \left[-\frac{5}{16r^5\phi'} - \frac{9\phi''}{64r^4\phi'^2} + \frac{\phi'''}{24r^3\phi'^2} - \frac{\phi''^2}{16r^3\phi'^3} - \frac{\phi^{(iv)}}{96r^2\phi'^2} + \frac{\phi''\phi'''}{24r^2\phi'^3} - \frac{\phi''^3}{32r^2\phi'^4} - \frac{\phi^{(vi)}}{576\phi'^2} + \frac{29\phi''\phi^{(v)}}{2880\phi'^3} + \frac{47\phi'''\phi^{(iv)}}{2880\phi'^3} - \frac{53\phi''^2\phi^{(iv)}}{1440\phi'^4} - \frac{7\phi''\phi'''^2}{144\phi'^4} + \frac{7\phi''^3\phi'''}{72\phi'^5} - \frac{7\phi''^5}{192\phi'^6}\right] \tag{2.2-2}$$

$$+\int_V^Q dr \left[-\frac{7}{1536}\phi''^2 (E-\phi)^{-\frac{7}{2}} + \left[-\frac{\phi''}{128 r^2} - \frac{\phi^{(IV)}}{768} \right] (E-\phi)^{-\frac{5}{2}} - \frac{5}{128 r^4} (E-\phi)^{-\frac{3}{2}} \right]$$

$$+\left[\frac{5}{64 r^4 \phi'} + \frac{\phi''}{48 r^3 \phi'^2} + \frac{\phi''^2}{96 r^2 \phi'^3} - \frac{\phi^{(V)}}{576 \phi'^2} - \frac{\phi'''}{96 r^2 \phi'^2} + \frac{19 \phi'' \phi^{(IV)}}{2880 \phi'^3} + \frac{7 \phi''^2}{1440 \phi'^3} - \frac{49 \phi'^2 \phi'''}{2880 \phi'^4} + \frac{7 \phi''^4}{960 \phi'^5} \right] (E-\phi)^{-\frac{1}{2}} \Bigg|_V^Q$$

$$+\left[\frac{\phi''}{192 r^2 \phi'} + \frac{\phi^{(IV)}}{1152 \phi'} + \frac{7 \phi''^3}{5760 \phi'^3} - \frac{7 \phi'' \phi'''}{2880 \phi'^2} \right] (E-\phi)^{-\frac{3}{2}} + \frac{7 \phi''^2}{3840 \phi'} (E-\phi)^{-\frac{5}{2}}$$

$$\frac{1}{n}\chi_{no} = \left[\frac{\pi}{2} - L \int_{r_3, r_1}^{\infty, r_2} dr\, r^{-2} (E-\phi)^{-\frac{1}{2}} \right] \qquad (2.2\text{-}3)$$

$$\frac{1}{n}\chi'_{no} = \int_{r_3, r_1, Q}^{\infty, V, r_2} dr\, (E-\phi)^{-\frac{1}{2}} \times \left[-\frac{1}{r^2} - \frac{8L^2}{r^5 \phi'} - \frac{2L^2 \phi''}{r^4 \phi'^2} \right] \qquad (2.2\text{-}4)$$

$$- \int_V^Q dr \left[\frac{1}{r^2} (E-\phi)^{-\frac{1}{2}} + \frac{L^2}{r^4} (E-\phi)^{-\frac{3}{2}} \right] + \frac{2L^2}{r^4 \phi'} (E-\phi)^{-\frac{1}{2}} \Bigg|_V^Q$$

$$\frac{1}{n}\chi''_{no} = -\int_{r_3, r_1, Q}^{\infty, V, r_2} dr\ (E-\phi)^{-\frac{1}{2}} \times \tag{2.2-5}$$

$$\times\left[\frac{24L}{r^5\phi'} + \frac{6L\phi''}{r^4\phi'^2} + \frac{168L^3}{r^8\phi'^2} + \frac{72L^3\phi''}{r^7\phi'^3} + \frac{12L^3\phi''^2}{r^6\phi'^4} - \frac{4L^3\phi'''}{r^6\phi'^3}\right]$$

$$-\int_V^Q dr\left[\frac{3L}{r^4}(E-\phi)^{-\frac{3}{2}} + \frac{3L^3}{r^6}(E-\phi)^{-\frac{5}{2}}\right]$$

$$+\left.\frac{2L^3}{r^6\phi'}(E-\phi)^{-\frac{3}{2}} + \left(\frac{6L}{r^4\phi'} + \frac{24L^3}{r^7\phi'^2} + \frac{4L^3\phi''}{r^6\phi'^3}\right)(E-\phi)^{-\frac{1}{2}}\right|_V^Q$$

$$\frac{1}{n}\psi_{no} = \frac{L}{12}\int_{r_3, r_1, Q}^{\infty, V, r_2} dr\ r^{-2}(E-\phi)^{-\frac{1}{2}} \times \tag{2.2-6}$$

$$\times\left[\frac{36}{r^3\phi'} + \frac{15\phi''}{r^2\phi'^2} + \frac{6\phi''^2}{r\phi'^3} - \frac{4\phi'''}{r\phi'^2} - \frac{4\phi''\phi'''}{\phi'^3} + \frac{3\phi''^3}{\phi'^4} + \frac{\phi^{(IV)}}{\phi'^2}\right]$$

$$+\frac{3}{4}\int_V^Q dr\left[\frac{\phi''}{r^2}(E-\phi)^{-\frac{5}{2}} + \frac{6}{r^4}(E-\phi)^{-\frac{3}{2}}\right]$$

$$-\left.\left(\frac{9}{r^4\phi'} + \frac{2\phi''}{r^3\phi'^2} + \frac{\phi''^2}{r^2\phi'^3} - \frac{\phi'''}{r^2\phi'^2}\right)(E-\phi)^{-\frac{1}{2}} - \frac{\phi''}{2r^2\phi'}(E-\phi)^{-\frac{3}{2}}\right|_V^Q$$

$$\frac{1}{n}\varphi_{no} = \int_{r_3, r_1, Q}^{\infty, V, r_2} dr\ (E-\phi)^{-\frac{1}{2}} \times \qquad (2.2\text{-}7)$$

$$\times\Bigg[-\frac{469L}{16r^8\phi'^2} - \frac{353L\phi''}{16r^7\phi'^3} + \frac{523L\phi'''}{96r^2\phi'^3}$$

$$-\frac{1169L\phi''^2}{96r^6\phi'^4} - \frac{71L\phi''^3}{12r^5\phi'^5} + \frac{6L\phi''\phi'''}{r^5\phi'^4}$$

$$-\frac{31L\phi^{(iv)}}{30r^5\phi'^3} - \frac{5L\phi''^4}{2r^4\phi'^6} - \frac{2L\phi'''^2}{3r^4\phi'^4}$$

$$+\frac{193L\phi''^2\phi'''}{48r^4\phi'^5} - \frac{247L\phi''\phi^{(iv)}}{240r^4\phi'^4} + \frac{17L\phi^{(v)}}{120r^4\phi'^3}$$

$$-\frac{49L\phi''^5}{48r^3\phi'^7} + \frac{7L\phi''^3\phi'''}{3r^3\phi'^6} - \frac{35L\phi''\phi'''^2}{36r^3\phi'^5}$$

$$-\frac{53L\phi''^2\phi^{(iv)}}{72r^3\phi'^5} + \frac{47L\phi'''\phi^{(iv)}}{180r^3\phi'^4} + \frac{29L\phi''\phi^{(v)}}{180r^3\phi'^4}$$

$$-\frac{L\phi^{(vi)}}{48r^3\phi'^3} - \frac{49L\phi''^6}{96r^2\phi'^8} + \frac{49L\phi''^4\phi'''}{32r^2\phi'^7}$$

$$-\frac{77L\phi''^2\phi'''^2}{72r^2\phi'^6} - \frac{9L\phi''^3\phi^{(iv)}}{16r^2\phi'^6} + \frac{37L\phi''^2\phi^{(v)}}{240r^2\phi'^5}$$

$$+\frac{17L\phi''\phi'''\phi^{(iv)}}{36r^2\phi'^5} - \frac{19L\phi'''\phi^{(v)}}{360r^2\phi'^4} - \frac{11L\phi''\phi^{(vi)}}{360r^2\phi'^4}$$

$$-\frac{47L\phi^{(iv)2}}{1440r^2\phi'^4} + \frac{7L\phi'''^3}{72r^2\phi'^5} + \frac{L\phi^{(viii)}}{288r^2\phi'^3}\Bigg]$$

$$+\int_V^Q d\tau \left[-\frac{67L}{128\tau^6}(E-\phi)^{-\frac{5}{2}} - \frac{49L\phi''^2}{1536\tau^2}(E-\phi)^{-\frac{9}{2}} \right.$$
$$\left. -\left(\frac{19\phi''}{128\tau^4} + \frac{5L\phi^{(IV)}}{768\tau^2}\right)(E-\phi)^{-\frac{7}{2}} \right]$$

$$+\left[\frac{67L}{16\tau^7\phi'^2} + \frac{73L\phi''}{32\tau^6\phi'^3} + \frac{16L\phi''^2}{15\tau^5\phi'^4} \right.$$
$$-\frac{19L\phi'''}{30\tau^5\phi'^3} + \frac{33L\phi''^3}{80\tau^4\phi'^5} - \frac{59L\phi''\phi'''}{120\tau^4\phi'^4}$$
$$+\frac{L\phi^{(IV)}}{10\tau^4\phi'^3} + \frac{7L\phi''^4}{48\tau^3\phi'^6} - \frac{49L\phi''^2\phi'''}{180\tau^3\phi'^5}$$
$$+\frac{7L\phi'''^2}{120\tau^3\phi'^4} + \frac{19L\phi''\phi^{(IV)}}{240\tau^3\phi'^4} - \frac{L\phi^{(V)}}{72\tau^3\phi'^3}$$
$$-\frac{29L\phi''\phi^{(V)}}{1440\tau^2\phi'^4} + \frac{L\phi^{(VI)}}{288\tau^2\phi'^3} - \frac{47L\phi'''\phi^{(IV)}}{1440\tau^2\phi'^4}$$
$$+\frac{53L\phi''^2\phi^{(IV)}}{720\tau^2\phi'^5} + \frac{7L\phi''\phi'''^2}{72\tau^2\phi'^5}$$
$$\left. -\frac{7L\phi''^3\phi'''}{36\tau^2\phi'^6} + \frac{7L\phi''^5}{96\tau^2\phi'^7} \right](E-\phi)^{-\frac{1}{2}} \Bigg|_V^Q$$

$$+\Bigg[+\frac{67L}{192r^6\phi'}+\frac{19L\phi''}{120r^5\phi'^2}+\frac{13L\phi''^2}{240r^4\phi'^3}$$

$$-\frac{19L\phi'''}{480r^4\phi'^2}+\frac{7L\phi''^3}{480r^3\phi'^4}+\frac{L\phi^{(iv)}}{288r^3\phi'^2}$$

$$-\frac{7L\phi''\phi'''}{360r^3\phi'^3}+\frac{7L\phi''^4}{960r^2\phi'^5}+\frac{7L\phi'''^2}{1440r^2\phi'^3}$$

$$-\frac{49L\phi''^2\phi'''}{2880r^2\phi'^4}+\frac{19L\phi''\phi^{(iv)}}{2880r^2\phi'^3}-\frac{L\phi^{(v)}}{576r^2\phi'^2}\Bigg](E-\phi)^{-\frac{3}{2}}$$

$$+\Bigg[\frac{19L\phi''}{320r^4\phi'}+\frac{7L\phi''^2}{960r^3\phi'^2}+\frac{7L\phi''^3}{1920r^2\phi'^3}$$

$$+\frac{L\phi^{(iv)}}{384r^2\phi'}-\frac{7\phi''\phi'''}{960r^2\phi'^2}\Bigg](E-\phi)^{-\frac{5}{2}}$$

$$+\frac{7L\phi''^2}{768r^2\phi'}(E-\phi)^{-\frac{7}{2}}$$

Q

V

The limits of integration for these functions are discussed in Chapter V.

The second complication is much more subtle and more laborious to overcome. The integration of $\eta_\ell^{(2)}$ and $\eta_\ell^{(3)}$ (and also the five functions Eqns. (2.2-3) through (2.2.-7)) between r_1 and r_2 (the turning points in the well. See Section 4 of Chapter V.) does not give zero as $r_2 - r_1$ goes to zero. That is, for a given energy these functions are discontinuous at a value of b such that $r_2 = r_1$. It becomes necessary, then, to modify the use of the Euler-Maclaurin approximation to take this discontinuity into account.

The discontinuity occurs, in general, for some non-integer value of ℓ , which shall be defined as ℓ' . The integer a is the first integer less than ℓ' and thus $a+1$ is the first integer greater than ℓ' . With these definitions it is possible to write $Q^{(1)}$ as

$$\frac{E\,Q^{(1)}}{4\pi} = \int_0^{a-1} (\ell+1)\sin^2(\eta_{\ell+1}-\eta_\ell)\,d\ell \qquad (2.2\text{-}8)$$
$$+ \text{Euler-Maclaurin terms}\Big|_0^{a-1}$$
$$+ (a+1)\sin^2(\eta_{a+1}-\eta_a)$$
$$+ \int_{a+1}^{\infty} (\ell+1)\sin^2(\eta_{\ell+1}-\eta_\ell)\,d\ell$$
$$+ \text{Euler-Maclaurin terms}\Big|_{a+1}^{\infty}$$

If the definition of Eqn. (2.1-5) is used to define an L', Eqn. (2.2-8) can be written

$$\frac{E Q^{(1)}}{4\pi} = \int_{\frac{1}{2}h}^{L'} R_\ell^{(1)} \sin^2(\eta_{\ell+1} - \eta_\ell) \frac{dL}{h} \qquad (2.2\text{-}9)$$

$$- \int_{(a-\frac{1}{2})h}^{L'} R_\ell^{(1)} \sin^2(\eta_{\ell+1} - \eta_\ell) \frac{dL}{h}$$

$$+ \int_{L'}^{\infty} R_\ell^{(1)} \sin^2(\eta_{\ell+1} - \eta_\ell) \frac{dL}{h}$$

$$- \int_{L'}^{(a+\frac{3}{2})h} R_\ell^{(1)} \sin^2(\eta_{\ell+1} - \eta_\ell) \frac{dL}{h}$$

$$+ \text{Euler-Maclaurin terms} \Big|_{\frac{1}{2}h}^{(a-\frac{1}{2})h}$$

$$+ \text{Euler-Maclaurin terms} \Big|_{(a+\frac{3}{2})h}^{\infty}$$

$$+ (a+1) \sin^2(\eta_{a+1} - \eta_a)$$

where $R_\ell^{(1)}$ is

$$R_\ell^{(1)} = \frac{L}{h} + \frac{1}{2} \qquad (2.2\text{-}10)$$

This procedure gives for $Q^{(2)}$

$$\frac{E Q^{(2)}}{2\pi} = \int_{\frac{3}{2}h}^{L'} R_\ell^{(2)} \sin^2(\eta_{\ell+2} - \eta_\ell) \frac{dL}{h} \qquad (2.2\text{-}11)$$

$$- \int_{(a-\frac{3}{2})h}^{L'} R_\ell^{(2)} \sin^2(\eta_{\ell+2} - \eta_\ell) \frac{dL}{h}$$

$$+\int_{L'}^{\infty} R_\ell^{(2)} \sin^2(\eta_{\ell+2}-\eta_\ell)\,\frac{dL}{h}$$

$$-\int_{L'}^{(a+\frac{3}{2})h} R_\ell^{(2)} \sin^2(\eta_{\ell+2}-\eta_\ell)\,\frac{dL}{h}$$

$$+\text{Euler-Maclaurin terms}\Big|_{\frac{3}{2}h}^{(a-\frac{3}{2})h}$$

$$+\text{Euler-Maclaurin terms}\Big|_{(a+\frac{3}{2})h}^{\infty}$$

$$+\frac{a(a+1)}{(a+\frac{1}{2})} \sin^2(\eta_{a+1}-\eta_{a-1})$$

$$+\frac{(a+1)(a+2)}{(a+\frac{3}{2})} \sin^2(\eta_{a+2}-\eta_a)$$

where

$$R_\ell^{(2)} = \frac{L}{h}\left(\frac{1+2\frac{h}{L}+\frac{3}{4}\left(\frac{h}{L}\right)^2}{1+\frac{h}{L}}\right) \qquad (2.2\text{-}12)$$

The Euler-Maclaurin terms at $L=\frac{1}{2}h$ for $Q^{(1)}$, $L=\frac{3}{2}h$ for $Q^{(2)}$, and $L=\infty$ for both, are evaluated in the same manner as for the monotonic potential and the same results are obtained. For the integrals in the range $((a-\frac{1}{2})h, L')$ for $Q^{(1)}$ and $((a-\frac{3}{2})h, L')$ for $Q^{(2)}$, and the Euler-Maclaurin terms evaluated at $(a-\frac{1}{2})h$ for $Q^{(1)}$ and $(a-\frac{3}{2})h$ for $Q^{(2)}$ it is necessary to expand the integrals about $L'^{(-)}$ (that is, the left hand limit) as they were expanded about $L=0$ for the

monotonic potential. Likewise, for the integrals in the range $(L', (a+\frac{3}{2})h)$ for $Q^{(1)}$, and $(L', (a+\frac{3}{2})h)$ for $Q^{(2)}$, and the Euler-Maclaurin terms evaluated at $(a+\frac{3}{2})h$ for $Q^{(1)}$ and $(a+\frac{3}{2})h$ for $Q^{(2)}$, it is necessary to expand the integrands about $L'^{(+)}$ (the right hand limit). The evaluation of these terms is carried out in a manner similar to that for the monotonic potential in Appendix I and are not repeated here.

The terms extracted from the sums in Eqns. (2.1-1) and (2.1-2) are treated in a slightly different manner. Since the phase shifts involved in the difference are on different "sides" of the discontinuity, it is impossible to make the same type of expansion as is used in Eqn. (16) of Appendix I. Instead, each phase shift is expanded about $L'^{(+)}$ or $L'^{(-)}$ depending, of course, on which side of the discontinuity it is. The difference between the two phase shifts, e.g. $\eta_{a+1} - \eta_a$ is

$$\eta_{a+1} - \eta_a = \sum_{i=0}^{\infty} h^{i-1} \left(\tilde{\chi}^{(+)}_{n,i-1} - \tilde{\chi}^{(-)}_{n,i-1} \right) \qquad (2.2\text{-}13)$$

(This expression is to be compared with Eqn. (18) of Appendix I) where

$$\tilde{\chi}^{(+)}_{n,i-1} = \sum_{k=1}^{1+\frac{i}{2}} \frac{(1+a-l')^{i-2k+2}}{(i-2k+2)!} \frac{\partial^{i-2k+2}}{\partial L^{i-2k+2}} \eta_l^{(k,+)} \qquad (2.2\text{-}14)$$

and

$$\tilde{\chi}^{(-)}_{n,i-1} = \sum_{k=1}^{1+\frac{1}{2}i} \frac{(a-l')^{i-2k+2}}{(i-2k+2)!} \frac{\partial^{i-2k+2}}{\partial L^{i-2k+2}} \eta_l^{(k,-)} \qquad (2.2\text{-}15)$$

(These last two expressions are to be compared with Eqn. (19) of Appendix I.)

The integer a is a function of h in a very complicated manner; so complicated in fact that it is impossible to incorporate its dependence into the series development. To avoid this difficulty we say that on the average

$$a = l' - \frac{1}{2} \qquad (2.2\text{-}16)$$

That is, if all possible values of the energy for which three turning points exist are considered, the discontinuity would occur, on the average, half way between two integer values of the angular momentum quantum number. With this definition it is possible to obtain expressions for $Q^{(1)}$ and $Q^{(2)}$ as series in h. In particular $Q^{(1)}$ becomes

$$Q^{(1)} = Q^{(1)}_{\text{monotonic}} \qquad (2.2\text{-}17)$$

$$+ h \frac{4\pi}{E} L' \left\{ \sin^2\left[\frac{1}{2}(\chi^{(+)}_{10} + \chi^{(-)}_{10}) - \frac{1}{2}(\sin^2\chi^{(+)}_{10} + \sin^2\chi^{(-)}_{10})\right\}\right.$$

$$+h^2\frac{4\pi}{E}\Bigg[\begin{aligned}&L'\left[\tfrac{1}{8}\left(\chi_{10}'^{(+)}-\chi_{10}'\right)+\eta_\ell^{(2,+)}-\eta_\ell^{(2,-)}\right]\sin\left(\chi_{10}^{(+)}+\chi_{10}^{(-)}\right)\\&-\frac{1}{8}\left(L'\chi_{10}'^{(+)}+1\right)\sin^2\chi_{10}^{(+)}\\&+\frac{1}{8}\left(L'\chi_{10}'^{(-)}+1\right)\sin^2\chi_{10}^{(-)}\\&+\frac{1}{2}L'\left(\chi_{10}'^{(-)}\sin 2\chi_{10}^{(-)}-\chi_{10}'^{(+)}\sin 2\chi_{10}^{(+)}\right)\end{aligned}\Bigg]$$

$$+h^3\frac{\pi}{E}L'\Bigg[\begin{aligned}&\left(\tfrac{1}{6}\chi_{10}''^{(+)}-2\psi_{10}^{(+)}\right)\sin 2\chi_{10}^{(+)}\\&-\left(\tfrac{1}{6}\chi_{10}''^{(-)}+2\psi_{10}^{(-)}\right)\sin 2\chi_{10}^{(-)}\\&+\left[\tfrac{1}{4}\left(\chi_{10}'^{(+)}-\chi_{10}'^{(-)}\right)+2\left(\eta_\ell^{(2,+)}-\eta_\ell^{(2,-)}\right)\right]^2\times\\&\quad\times\cos\left(\chi_{10}^{(+)}+\chi_{10}^{(-)}\right)\\&+\left[\frac{1}{12}\left(\chi_{10}''^{(+)}+\chi_{10}''^{(-)}\right)+2\left(\psi_{10}^{(+)}+\psi_{10}^{(-)}\right)\right]\times\\&\quad\times\sin\left(\chi_{10}^{(+)}+\chi_{10}^{(-)}\right)\end{aligned}\Bigg]$$

$$
+h^4\frac{\pi}{E}\Bigg[
\begin{bmatrix} -\frac{1}{24}L(\chi_{10}'^{(+)})^3+\frac{25}{96}\chi_{10}''^{(+)}-\frac{1}{96}L'\chi_{10}''^{(+)} \\ -\frac{1}{4}\psi_{10}^{(+)}-\frac{1}{2}L'\psi_{10}'^{(+)} \end{bmatrix}\sin 2\chi_{10}^{(+)}
$$

$$
+\begin{bmatrix} -\frac{7}{24}L'(\chi_{10}'^{(-)})^3+\frac{23}{96}\chi_{10}''^{(-)}+\frac{13}{96}L'\chi_{10}'''^{(-)} \\ +\frac{1}{2}\psi_{10}^{(-)}+\frac{1}{2}L'\psi_{10}' \end{bmatrix}\sin 2\chi_{10}^{(-)}
$$

$$
+\begin{bmatrix} \frac{7}{24}(\chi_{10}'^{(+)})^2-\frac{7}{48}L'\chi_{10}'^{(+)}\chi_{10}''^{(+)} \\ -L'\chi_{10}'^{(+)}\psi_{10}^{(+)} \end{bmatrix}\cos 2\chi_{10}^{(+)}
$$

$$
+\begin{bmatrix} \frac{3}{8}(\chi_{10}'^{(-)})^2-\frac{121}{48}L'\chi_{10}'^{(-)}\chi_{10}''^{(-)} \\ +L'\chi_{10}'^{(-)}\psi_{10}^{(-)} \end{bmatrix}\cos 2\chi_{10}^{(-)}
$$

$$
+L'\begin{bmatrix} \left[(\chi_{10}'^{(+)}-\chi_{10}'^{(-)})+4(\eta_\ell^{(2,+)}-\eta_\ell^{(2,-)}\right]\times \\ \times\left[\frac{1}{48}(\chi_{10}''^{(-)}-\chi_{10}''^{(+)})+\frac{1}{2}(\psi_{10}^{(-)}-\psi_{10}^{(+)})\right] \end{bmatrix}\cos(\chi_{10}^{(+)}+\chi_{10}^{(-)})
$$

$$
+L'\Bigg[\begin{bmatrix} \frac{1}{96}(\chi_{10}'''^{(+)}-\chi_{10}'''^{(-)})+\frac{1}{8}(\psi_{10}'^{(+)}-\psi_{10}'^{(-)}) \\ +(\eta_\ell^{(3,+)}-\eta_\ell^{(3,-)}-\frac{2}{3}\left(\frac{1}{8}\chi_{10}'^{(+)}+\eta_\ell^{(2,+)}\right)^3 \\ +\frac{2}{3}\left(\frac{1}{8}\chi_{10}'^{(-)}+\eta_\ell^{(2,-)}\right)^3 \end{bmatrix}\sin(\chi_{10}^{(+)}+\chi_{10}^{(-)})\Bigg]
$$

The series for $Q^{(2)}$ is disappointing in that the terms in $\hbar^3$ and $\hbar^4$ can not be summed. The term involved in the term analogous to the logarithm in Eqn. (49) of Appendix I. Explicitly, $Q^{(2)}$ becomes, to terms in $\hbar^4$,

$$
\begin{aligned}
Q^{(2)} = \; & Q^{(2)}_{\text{monotonic}} \qquad (2.2\text{-}18)\\
& + \hbar \frac{\pi}{E} L' \left[\begin{array}{l} -\sin^2 \chi^{(+)}_{20} - 3\sin^2 \chi^{(-)}_{20} \\ +2\sin^2\left(\frac{3}{2}\chi^{(+)}_{20} + \frac{1}{2}\chi^{(-)}_{20}\right) \\ +2\sin^2\left(\frac{1}{2}\chi^{(+)}_{20} + \frac{3}{2}\chi^{(-)}_{20}\right) \end{array} \right] \\
& + \hbar^2 \frac{\pi}{E} \left[\begin{array}{l} -\frac{3}{4} L' \chi'^{(+)}_{20} \sin 2\chi^{(+)}_{20} + 6\sin^2 \chi^{(-)}_{20} \\ +\left[\frac{1}{8}\left(9\chi'^{(+)}_{20} - \chi'^{(-)}_{20}\right) + \eta_\ell^{(2,+)} - \eta_\ell^{(2,-)}\right] \times \\ \times \sin\left(3\chi^{(+)}_{20} + \chi^{(-)}_{20}\right) + \frac{3}{4} L' \chi'_{20} \sin 2\chi^{(-)}_{20} \\ +\left[\frac{1}{8}\left(\chi'^{(+)}_{20} - 9\chi'^{(-)}_{20}\right) + \left(\eta_\ell^{(2,+)} - \eta_\ell^{(2,-)}\right)\right] \times \\ \times \sin\left(\chi^{(+)}_{20} + 3\chi^{(-)}_{20}\right) \\ +\frac{1}{2}\sin^2\left(\frac{3}{2}\chi^{(+)}_{20} + \frac{1}{2}\chi^{(-)}_{20}\right) \\ +\frac{3}{2}\sin^2\left(\frac{1}{2}\chi^{(+)}_{20} + \frac{3}{2}\chi^{(-)}_{20}\right) \end{array} \right]
\end{aligned}
$$

These expressions are valid only when the energy is such that three turning points are possible. For other energies (that is, energies above the critical value, below which there can be three

turning points and above which there can only be one) the expressions for $Q^{(1)}$ and $Q^{(2)}$ are those given in Eqns. (2.1-14) and (2.1.-15). However, the expressions for χ_{no}, χ'_{no}, χ''_{no}, ψ_{no}, and ϑ_{no} given by Eqns. (2.2-3) through (2.2-7) must be used because of the ϕ' that appears in the denominator of these integrands.

The added contributions for potentials with a minimum are rather puzzling because they give contributions from just one point on the trajectory. Also, these contributions introduce terms in $\hbar$ and $\hbar^3$.

3. The Quantum Corrections to the Omega Integrals and the Transport Coefficients.

The omega integrals[16] are defined as

$$\Omega^{(l,s)}(T) = \frac{1}{2}\sqrt{\frac{\kappa T}{2\pi\mu}}\,\frac{1}{(\kappa T)^{s+2}}\int_0^\infty e^{-\frac{E}{\kappa T}} E^{s+1} Q^{(l)}(E)\,dE \quad (2.3\text{-}1)$$

where μ is the reduced mass of the colliding particles, T is the temperature and κ is Boltzmann's constant.

The series for $Q^{(l)}$ makes it possible to write $\Omega^{(l,s)}$ as a series in $\hbar$. For convenience, the series for $Q^{(l)}$ is written as

$$Q^{(l)} = Q_{CL}^{(l)} + \hbar\, Q_{I}^{(l)} + \hbar^2 Q_{II}^{(l)} + \hbar^3 Q_{III}^{(l)} + \hbar^4 Q_{IV}^{(l)} + \cdots \quad (2.3\text{-}2)$$

for ℓ = 1 and 2 . Substitution of this series into the expression for $\Omega^{(\ell,s)}$ gives

$$\Omega^{(\ell,s)} = \Omega_{CL}^{(\ell,s)} + h\Omega_{I}^{(\ell,s)} + h^2\Omega_{II}^{(\ell,s)} + h^3\Omega_{III}^{(\ell,s)} + h^4\Omega_{IV}^{(\ell,s)} + \cdots \tag{2.3-3}$$

where

$$\Omega_{i}^{(\ell,s)} = \frac{1}{2(kT)^{s+1}}\sqrt{\frac{kT}{2\pi\mu}}\int_0^\infty e^{-\frac{E}{kT}} E^{s+1} Q_i^{(\ell)}(E)\,dE \tag{2.3-4}$$

and the subscript i represents CL , I , II , III , or IV.

The transport coefficients, self diffusion, $\mathcal{D}$, viscosity, η , and thermal conductivity, λ , may be written in terms of the omega integrals.[17] Explicitly,

$$\mathcal{D} = \frac{3kT}{8\rho\Omega^{(1,1)}}$$

$$\eta = \frac{5kT}{8\Omega^{(2,2)}} \tag{2.3-5}$$

$$\lambda = \frac{25C_v kT}{16\Omega^{(2,2)}}$$

where ρ is the density and C_v is the specific heat at constant volume per unit mass.

Formally, this is as far as the treatment can be taken. In order to proceed to numerical results an intermolecular potential must be specified.

CHAPTER III

THE SQUARE WELL

Before proceeding to the evaluation of the expressions obtained in Chapter II for a realistic intermolecular potential, a simple model potential that demonstrates some of the important points of the theory is treated.

1. The Potential

The potential used in the square well potential defined by

$$\varphi = -\epsilon \qquad r \leq \sigma$$
$$\varphi = 0 \qquad r > \sigma \tag{3.1.-1}$$

The effective potential, which is defined as

$$\phi = \varphi + \frac{L^2}{r^2} \tag{3.1-2}$$

is plotted along with φ in Figure (3-1).

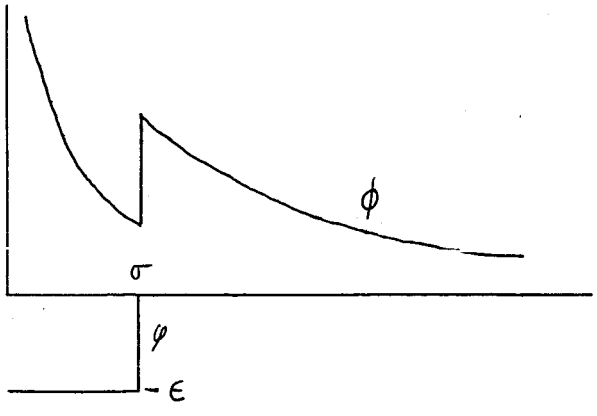

Figure 3-1

This potential has two features which demonstrate the properties of the three turning point problem: (1) it is zero beyond $r = \sigma$ and thus the role of the centrifugal potential is not modified by the potential itself, (2) the limiting expressions for $Q^{(1)}$ and $Q^{(2)}$ can be evaluated exactly.

2. The Range of the r Integration

In analyzing the dynamics of a two body collision using classical mechanics, a quantity called the angle of deflection is defined. It is the angle through which the relative velocity vector turns as the particles come in from infinity, collide, and go out to infinity again. The angle of deflection is given by the expression

$$\chi = \pi - 2L \int dr \; r^{-2} (E - \phi)^{-\frac{1}{2}} \qquad (3.2\text{-}1)$$

where the range of the integration on r is from the distance of closest approach of the particles to infinity. That is, over one-half of the trajectory. The distance of closest approach is the largest positive root of $E - \phi$. This expression defines the point where the total energy of the colliding particles E is all in the potential energy of interaction and the centrifugal potential. At this point on the trajectory the radial velocity becomes zero, the radial velocity vector reverses direction, and the particles begin to separate.

From Fig. (3-1), however, it is seen that for some values of the energy there are three positive roots of $E-\phi=0$. The largest root is again the classical turning point. The two lesser roots are the turning points of a particle trapped in the potential well. When only two body, classical collisions are permitted, particles trapped in the well cannot leave and no particles can get into the well.

The quantum mechanical treatment of the dynamics of a two body collision introduces the possibility of tunnelling through the barrier into the inner region. In the Curtiss-Powers semi-classical treatment of this problem it is found that the inner region does contribute in a manner analogous to the outer region. That is, to obtain the quantity χ of Eqn. (3.2-1) (and all other quantities integrated over the trajectory) it is necessary to integrate from r_1 to r_2 and from r_3 to infinity, where r_1, r_2, and r_3 are the three roots of $E-\phi=0$ with $r_1 < r_2 < r_3$. Moreover, even in the limit as $\hbar$ goes to zero the integration over the inner region contributes.

It is convenient at this point to differentiate between this limit and the purely classical result. In this work an expression is called "classical" (and labelled with the subscript cl) if it is derived from classical mechanics. An expression is called a "classical limit" (and labelled with the subscript CL) if it is the limit as $\hbar$ goes to zero of a semi-classical treatment.

The effect of this inner region is considered by comparing the classical, classical limit, and the quantum expressions for $Q^{(1)}$ and $Q^{(2)}$.

3. The Classical Expression for $Q^{(1)}$ and $Q^{(2)}$.

In order to obtain expressions for $Q^{(1)}$ and $Q^{(2)}$, the first and second moments of the cross section, it is necessary to obtain an expression for the cross section itself. The differential cross section is defined[18] as

$$\sigma(E,\chi) = \left| \frac{b}{\sin\chi} \cdot \frac{db}{d\chi} \right| \tag{3.3-1}$$

where χ is the angle of deflection of the collision and b is defined as $\frac{L}{\sqrt{E}}$. In a geometric sense, b is the distance at which the two particles would pass each other if the potential of interaction was zero. The angle of deflection is calculated using Eqn. (3.2-1). Since the range of the potential is σ, particles with an impact parameter greater than σ pass each other without effect. For $b \leq \sigma$, the angle of deflection is

$$\chi = \pi - 2b\int_{\frac{b}{(1+\frac{\epsilon}{E})^{\frac{1}{2}}}}^{\sigma} dr\, r^{-2}\left(1+\frac{\epsilon}{E}-\frac{b^2}{r^2}\right)^{-\frac{1}{2}} - 2b\int_{\sigma}^{\infty} dr\, r^{-2}\left(1-\frac{b^2}{r^2}\right)^{-\frac{1}{2}} \tag{3.3-2}$$

Further, a dimensionless parameter η is defined as

$$\eta \equiv \left(\frac{E+\epsilon}{E}\right)^{\frac{1}{2}} \tag{3.3-3}$$

The integrals are straightforward[19] and the expression for χ is found to be

$$\chi = 2\left[\arccos\left(\frac{b}{\sigma}\right) - \arccos\left(\frac{b}{\sigma n}\right)\right] \qquad (3.3\text{-}4)$$

This expression is inverted to give b as a function of χ .

$$\frac{b^2}{\sigma^2 n^2} = \frac{1 - \cos^2\frac{\chi}{2}}{1 + n^2 - 2n\cos\frac{\chi}{2}} \qquad (3.3\text{-}5)$$

Equation (3.3-4), (3.3-5), and (3.3-1) are combined to give

$$\sigma_{el}(\chi, n) = \frac{\sigma^2 n^2\left(n\cos\frac{\chi}{2} - 1\right)\left(n - \cos\frac{\chi}{2}\right)}{4\left(1 + n^2 - 2n\cos\frac{\chi}{2}\right)^2\cos\frac{\chi}{2}} \qquad (3.3\text{-}6)$$

as the expression for the classical differential cross section.

For the sake of completion (and also to show the effect of the inner region which is considered in detail in the next section), the total cross section is derived. The total cross section is defined[20] as the integral of the differential cross section over all angles

$$Q_{el} = \int \sigma(\chi, E)\, d\Omega \qquad (3.3\text{-}7)$$

Since $\sigma(\chi, E)$ is independent of the azimuthal angle this expression can be integrated to give

$$Q_{el} = 2\pi \int_0^{|\chi_{b=\sigma}|} \sigma(\chi, E) \sin\chi \, d\chi \qquad (3.3\text{-}8)$$

The upper limit of the integration is found by considering the angle of deflection in a collision where $b = \sigma$. From Eqn. (3.3-4),

$$\chi_{b=\sigma} = -2 \arccos \frac{1}{n} \qquad (3.3\text{-}9)$$

Therefore, Q_{el} becomes

$$Q_{el} = \pi\sigma^2 n^2 \int_0^{2\arccos\frac{1}{n}} \frac{(n\cos\frac{\chi}{2} - 1)(n - \cos\frac{\chi}{2})}{(1 + n^2 - 2n\cos\frac{\chi}{2})^2} \sin\frac{\chi}{2} d\chi \qquad (3.3\text{-}10)$$

To complete the integration let

$$x = \cos\frac{\chi}{2} \qquad (3.3\text{-}11)$$

then

$$dx = -\frac{1}{2}\sin\frac{\chi}{2}\, d\chi \qquad (3.3\text{-}12)$$

At $\chi = 0$, $x = 1$; at $\chi = 2\arccos\frac{1}{n}$, $x = \frac{1}{n}$

The expression for Q_{el} is then

$$Q_{el} = 2\pi\sigma^2 n^2 \int_{\frac{1}{n}}^{1} \frac{(nx - 1)(n - x)}{(1 + n^2 - 2nx)^2} \, dx \qquad (3.3\text{-}13)$$

The numerator is expanded and the integrals evaluated.[21] After considerable algebra, the total cross section is found to be

$$Q_{el} = \pi \sigma^2 \tag{3.3-14}$$

This is to be expected since the potential is spherically symmetric and has a finite cutoff at $r = \sigma$.

The expression[22] for $Q_{el}^{(1)}$ in terms of the cross section is

$$Q_{el}^{(1)} = 4\pi \int_0^{2 \arccos \frac{1}{n}} \sin^2 \frac{\chi}{2}\, \sigma(n, \chi) \sin \chi \, d\chi \tag{3.3-15}$$

In terms of the change of variable given in Eqn. (3.3-11) $Q_{el}^{(1)}$ is

$$Q_{el}^{(1)} = 4\pi\sigma^2 n^2 \int_{\frac{1}{n}}^{1} \frac{(nx-1)(n-x)}{(1+n^2-2nx)^2}(1-x^2)\, dx \tag{3.3-16}$$

After considerable algebra it is found that

$$Q_{el}^{(1)} = \pi\sigma^2 \left[\frac{(n^2+1)(n^2-1)^2}{4n^2} \ln \left| \frac{n+1}{n-1} \right| - \frac{(n-1)^2(3n^3+6n^2+7n+2)}{6n^2} \right] \tag{3.3-17}$$

The expression[22] for $Q^{(2)}$ in terms of the cross section is

$$Q_{el}^{(2)} = 2\pi \int_0^{2\arccos\frac{1}{n}} \sin^3\chi\, \sigma(n,\chi)\, d\chi \qquad (3.3\text{-}18)$$

In terms of x this is

$$Q_{el}^{(2)} = 8\pi\sigma^2 n^2 \int_{\frac{1}{n}}^{1} \frac{(nx-1)(n-x)}{(1+n^2-2nx)^2} x^2(1-x^2)\, dx \qquad (3.3\text{-}19)$$

After even more algebra it is found that

$$Q_{el}^{(2)} = \pi\sigma^2 \left[\frac{(n^2-1)^2(n^2+)(n^4+1)}{4n^4} \ln\left|\frac{n+1}{n-1}\right| - \frac{(n-1)^2(15n^7+30n^6+35n^5+40n^4+43n^3+26n^2-n-8)}{60n^4} \right] \qquad (3.3\text{-}20)$$

The limiting forms of $Q_{el}^{(1)}$ and $Q_{el}^{(2)}$ for large and small $E^* = \frac{E}{\epsilon}$ are interesting. First, as $E^* \to \infty$, $n \to 1$. As can be easily seen from Eqns. (3.3-17) and (3.3-20)

$$\left.\begin{aligned} Q_{el}^{(1)} &\to 0 \\ Q_{el}^{(2)} &\to 0 \end{aligned}\right\} \text{ as } E^* \to \infty \qquad (3.3\text{-}21)$$

In the limit of small E^*, $n \to \infty$. The logarithm is expanded[23] in the series

$$\ln\left|\frac{n+1}{n-1}\right| = 2\sum_{i=0}^{\infty} \frac{1}{(2i+1)n^{2i+1}} \qquad (3.3\text{-}22)$$

and this series is used in Eqns. (3.3-17) and (3.3-20). The limiting forms are found to be

$$Q_{el}^{(1)} = \pi\sigma^2\left[1 - \frac{16}{15}E^{*\frac{1}{2}} - \frac{1}{3}E^{*} + \ldots\right] \tag{3.3-23}$$

$$Q_{el}^{(2)} = \frac{2}{3}\pi\sigma^2\left[1 + \frac{16}{35}E^{*\frac{1}{2}} - E^{*} + \ldots\right]$$

Thus, both $Q^{(1)}$ and $Q^{(2)}$ approach their respective rigid sphere values as $E^{*} \to 0$. The first moment, $Q^{(1)}$, approaches from below, while $Q^{(2)}$ approaches its rigid sphere value from above.

The approach to the rigid sphere limit can also be seen by examining the nature of the differential cross section in the low energy limit. Equation (3.3.-4) is rewritten to give

$$\cos\frac{\chi}{2} = \frac{b^2}{\sigma^2 n^2} + \left(1 - \frac{b^2}{\sigma^2}\right)^{\frac{1}{2}}\left(1 - \frac{b^2}{\sigma^2 n^2}\right)^{\frac{1}{2}} \tag{3.3-24}$$

This is substituted in Eqn. (3.3-6) to give

$$\sigma_{el} = \frac{\sigma^2 n^2\left[\frac{b^2}{\sigma^2} + \left(1 - \frac{b^2}{\sigma^2}\right)^{\frac{1}{2}}\left(n^2 - \frac{b^2}{\sigma^2}\right)^{\frac{1}{2}} - 1\right]}{4\left[1 + n^2 - 2\frac{b^2}{\sigma^2} - 2\left(1 - \frac{b^2}{\sigma^2}\right)^{\frac{1}{2}}\left(n^2 - \frac{b^2}{\sigma^2}\right)^{\frac{1}{2}}\right]^2} \times$$

$$\times \frac{\left[n^2 - \frac{b^2}{\sigma^2} - \left(1 - \frac{b^2}{\sigma^2}\right)^{\frac{1}{2}}\left(n^2 - \frac{b^2}{\sigma^2}\right)^{\frac{1}{2}}\right]}{\left[\frac{b^2}{\sigma^2} + \left(1 - \frac{b^2}{\sigma^2}\right)^{\frac{1}{2}}\left(n^2 - \frac{b^2}{\sigma^2}\right)^{\frac{1}{2}}\right]} \tag{3.3-25}$$

As $\eta \to \infty$ this expression reduces to

$$\sigma_{\eta \to \infty} = \frac{1}{4} \sigma^2 \qquad (3.3\text{-}26)$$

which is the rigid sphere limit.

4. The Classical Limit Expressions for $Q^{(1)}$ and $Q^{(2)}$.

The difference between the classical limit and the classical expressions in this problem is that the former includes the contribution of the inner region. Thus, the classical limit expressions for $Q^{(1)}$ and $Q^{(2)}$ are larger than the classical expressions for the same quantities by the addition of the effect of the tunnelling collisions.

Figure (3-2a) shows the collision region of the classical treatment. Figure (3-2b) shows the collision region of the classical limit treatment. That is, in the classical limit there is a

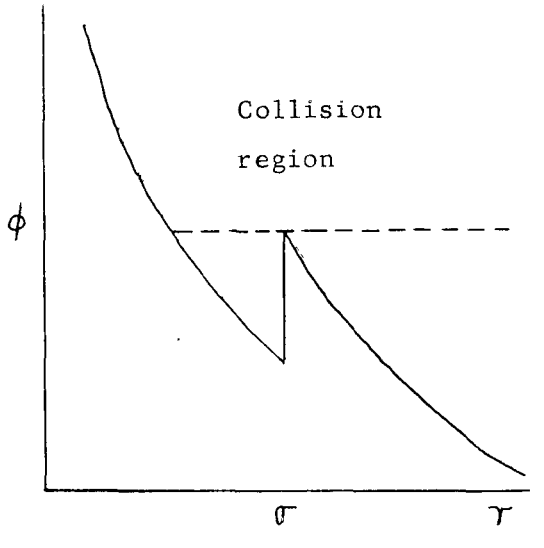

Figure 3-2a

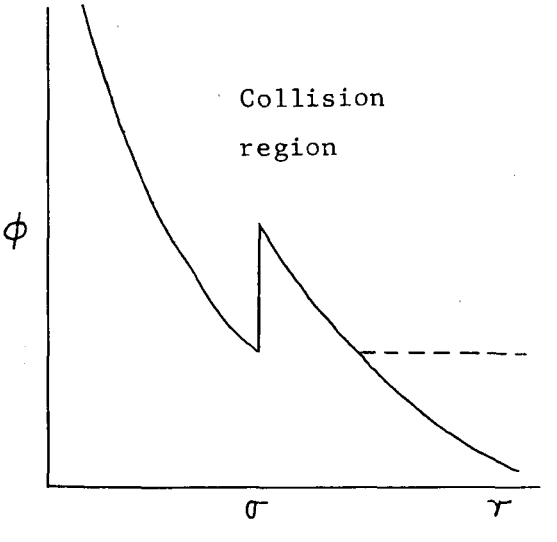

Figure 3-2b

contribution to the differential cross section for $b > \sigma$.

The contribution to the angle of deflection for tunnelling collisions is

$$\chi_t = \pi - 2b\int_b^\infty dr\, r^{-2}\left(1-\frac{b^2}{r^2}\right)^{-\frac{1}{2}} - 2b\int_{\frac{b}{n}}^{\sigma} dr\, r^{-2}\left(1+\frac{\epsilon}{E}-\frac{b^2}{r^2}\right)^{-\frac{1}{2}} \qquad \sigma < b \leq n\sigma$$

$$\chi_t = 0 \qquad b > n\sigma \qquad (3.4\text{-}1)$$

The integrals are straightforward and give for χ_t

$$\chi_t = -2\arccos\left(\frac{b}{\sigma n}\right) \qquad \sigma < b \leq n\sigma \qquad (3.4\text{-}2)$$

Thus, there is a contribution to χ in the classical limit for impact parameters as great as σn . The full classical limit expression for the angle of deflection is given by a combination of Eqn. (3.3-4) and (3.4-2).

$$\chi_{CL} = \begin{cases} 2\left[\arccos\left(\frac{b}{\sigma}\right) - \arccos\left(\frac{b}{\sigma n}\right)\right] & 0 < b \leq \sigma \\ -2\arccos\left(\frac{b}{\sigma n}\right) & \sigma < b \leq \sigma n \\ 0 & b > \sigma n \end{cases}$$

(3.4-3)

A plot of this function is given in Chapter VI. The curve is continuous at $b = \sigma$, but its slope is discontinuous.

The tunnelling contribution to the differential cross section is obtained by use of Eqns. (3.3-1) and (3.4-2). The expression is

$$\sigma_t = \frac{1}{4} \sigma^2 n^2 \qquad (3.4\text{-}4)$$

The fact that the tunnelling contribution to the differential cross section is independent of the impact parameter is rather interesting. In general, the differential cross section is a function of the energy and the impact parameter (the differential cross section is usually written as a function of the energy and the angle of deflection. However, since the angle of deflection is a post-collision property it seems more logical, in this case, to speak of the impact parameter, which is a pre-collision parameter. Since the two are related, e.g., by Eqn. (3.4-2), this preference is immaterial. It is usually easier to express χ as a function of $b)$. Equation (3.4-4) says, in effect, that if the impact parameter is between σ and σn , the probability of a particle being scattered into a solid angle $d\Omega$ is dependent only on the energy.

The tunnelling contribution to the total cross section is derived, as was the classical total cross section, by use of Eqns. (3.3-8) and (3.4-4). The limits of integration in this case are found from Eqn. (3.4-2). The expression for the tunnelling

total cross section is

$$Q_t = \pi\sigma^2(n^2-1) \tag{3.4-5}$$

The classical limit total cross section is the sum of Eqns. (3.3-14) and (3.4-5) and is

$$Q_{CL} = \pi\sigma^2 n^2 \tag{3.4-6}$$

Since σn is the largest impact parameter for which tunnelling can occur, the total cross section is represented in space as a circular area of radius σn, even though the potential cuts off at a distance σ. The fact that n goes to infinity as E^* goes to zero means that the cross section <u>expands</u> in this limit. This property of the tunnelling cross section has a strong effect on $Q^{(1)}$ and $Q^{(2)}$ in the low energy limit.

By use of Eqns. (3.3-15), (3.3-18), and (3.4-4), the tunnelling contributions to $Q^{(1)}$ and $Q^{(2)}$ are found to be

$$Q_t^{(1)} = \frac{\pi\sigma^2}{n^2}(n^2-1)^2 \tag{3.4-7}$$

$$Q_t^{(2)} = \frac{2\pi\sigma^2}{3n^4}(n^2-1)^2(n^2+2) \tag{3.4-8}$$

It will be noticed that as n approaches infinity (that is, as E^* approaches zero), both $Q^{(1)}$ and $Q^{(2)}$ go to infinity as n^2. These quantities, when added to (3.3-17) and (3.3-20) respectively make the classical limit quantities go to infinity as E^* goes to zero.

In the upper limit, that is, as E^* goes to infinity, $Q_t^{(1)}$ and $Q_t^{(2)}$ go to zero as $\frac{1}{E^{*2}}$. By way of contrast, $Q_{el}^{(1)}$ and $Q_{el}^{(2)}$ go to zero more slowly, as $\frac{1}{E^{*2}} \ln \frac{1}{E^*}$.

5. Quantum Expressions for $Q^{(1)}$ and $Q^{(2)}$.

Equations (2.1-1) and (2.1-2) of Chapter II give $Q^{(1)}$ and $Q^{(2)}$ in terms of the phase shifts. For the square well potential the phase shifts have been obtained by Mott and Massey.[24] Their result can be written in the form

$$\eta_l = \arctan(-1)^l \frac{\mathcal{H}'\sigma J_{l-\frac{1}{2}}(\mathcal{H}\sigma) J_{l+\frac{1}{2}}(\mathcal{H}'\sigma) + \mathcal{H}\sigma J_{l+\frac{1}{2}}(\mathcal{H}'\sigma) J_{l-\frac{1}{2}}(\mathcal{H}\sigma)}{\mathcal{H}\sigma J_{l+\frac{1}{2}}(\mathcal{H}'\sigma) J_{l+\frac{1}{2}}(\mathcal{H}\sigma) - \mathcal{H}'\sigma J_{l+\frac{1}{2}}(\mathcal{H}\sigma) J_{l+\frac{1}{2}}(\mathcal{H}'\sigma)} \tag{3.5-1}$$

where

$$\mathcal{H}'\sigma = \frac{2\pi}{\lambda^*}\sqrt{E^*+1}$$

and

$$\mathcal{H}\sigma = \frac{2\pi}{\lambda^*}\sqrt{E^*} \tag{3.5-2}$$

and Λ^* is defined by Eqn. (5.1-4). Because of the complexity of this expression, numerical procedures were used to obtain $Q_{qu}^{(1)}$ and $Q_{qu}^{(2)}$.

It is necessary, then, to compare $Q_{ee}^{(2)}$, $Q_{cL}^{(2)}$, and $Q_{qu}^{(2)}$ numerically. This procedure is explained in Chapter V.

CHAPTER IV

THE EFFECT OF THE ATTRACTIVE PART OF THE LENNARD-JONES (12,6) POTENTIAL ON THE TRANSPORT CROSS SECTIONS

The role of the attractive part of Lennard-Jones (12,6) potential in the quantum and semi-classical calculations of the transport cross-sections (particularly $Q^{(2)}$ has been debated for many years. One of the first quantum calculations of the transport cross-sections for the Lennard-Jones (12,6) potential was made by de Boer.[25] He carried out these calculations using the parameters for He^4. Because of limited computing facilities he was unable to extend his calculations beyond $E^* = 1.5$. He found that the quantal $Q^{(2)}$ was less than the pure classical $Q^{(2)}$ at every energy considered. In 1954 de Boer and Bird,[13] using the WKB method, obtained the first quantum correction to the transport cross-sections. They argued that at high energies only the repulsive part of the potential was important and so calculated the classical term and the first quantum correction for the r^{-12} potential. They found that for this potential their semi-classical $Q^{(2)}$ was higher than the classical $Q^{(2)}$ calculated using the Lennard-Jones (12,6) potential (again, the parameters for He^4 were used). They concluded, therefore, that the quantum and the pure classical curves crossed at about $E^* \sim 4$. In 1964 Munn, Smith and Mason[11] calculated the pure quantum $Q^{(2)}$ using the (12,6) potential and the parameters for He^4, out to $E^* = 16$. Their quantum $Q^{(2)}$ lies below the classical $Q^{(2)}$ at all computed

energies. They concluded therefore, that the crossover predicted by de Boer and Bird did not take place at $E^* = 4$; and that de Boer and Bird had extended their calculation to energies too low for the attractive part of the potential to be neglected. However, since the first quantum correction of de Boer and Bird is positive, Munn, Smith, and Mason concluded that the quantum $Q^{(2)}$ must cross the classical limit $Q^{(2)}$ at a much higher energy.

It is the purpose of this chapter to ascertain the influence of the attractive part of the potential on the classical limit and the first two quantum corrections to the transport properties. Also, since at very high energies the attractive portion of the Lennard-Jones (12,6) potential can be neglected, the expressions obtained in Chapter II can be checked at high energies.

1. The Perturbation

The attractive part of the Lennard-Jones (12,6) potential is taken to be a perturbation on the repulsive part. To effect an ordering of the perturbation series, a parameter, λ , is introduced into the potential, so that

$$\varphi = 4\epsilon\left[\left(\frac{\sigma}{r}\right)^{12} - \lambda\left(\frac{\sigma}{r}\right)^{6}\right] \qquad (4.1\text{-}1)$$

This parameter is eventually set equal to unity.

2. The Perturbation Expansion

The perturbation series is obtained by expanding the

expressions for the $Q^{(\ell)}$ (for a potential with a minimum) in a Taylor series about $\lambda = 0$. This series is valid only in the limit of high energy. Since the terms peculiar to the attractive potentials, Eqns. (2.2-17) and (2.2-18), are zero except at very low energies, they are neglected in this treatment. Therefore $Q^{(\ell)}$ can be written

$$Q^{(\ell)} = Q_{CL}^{(\ell)} + \hbar^2 Q_{II}^{(\ell)} + \hbar^4 Q_{IV}^{(\ell)} + \cdots \tag{4.2-1}$$

The perturbation series for $Q^{(\ell)}$ may be written as the double sum

$$Q^{(\ell)} = \sum_{j,k} \lambda^j \hbar^{2k} Q_{jk}^{(\ell)} \tag{4.2-2}$$

or explicitly in the expanded form

$$\begin{aligned} Q^{(\ell)} = {} & Q_{00}^{(\ell)} + \hbar^2 Q_{01}^{(\ell)} + \hbar^4 Q_{02}^{(\ell)} + \cdots \\ & + \lambda Q_{10}^{(\ell)} + \lambda \hbar^2 Q_{11}^{(\ell)} + \cdots \\ & + \lambda^2 Q_{20}^{(\ell)} + \cdots \\ & + \cdots \end{aligned} \tag{4.2-3}$$

where

$$Q_{00}^{(\ell)} = Q_{ee}^{(\ell)}\Big|_{\lambda=0} \qquad Q_{01}^{(\ell)} = Q_{II}^{(\ell)}\Big|_{\lambda=0}$$

$$Q_{10}^{(\ell)} = \frac{\partial Q_{ee}^{(\ell)}}{\partial \lambda}\Big|_{\lambda=0} \qquad Q_{11}^{(\ell)} = \frac{\partial Q_{II}^{(\ell)}}{\partial \lambda}\Big|_{\lambda=0} \tag{4.2-4}$$

$$Q_{20}^{(\ell)} = \frac{\partial^2 Q_{ee}^{(\ell)}}{\partial \lambda^2}\Big|_{\lambda=0} \qquad Q_{02}^{(\ell)} = Q_{IV}^{(\ell)}\Big|_{\lambda=0}$$

The explicit expressions for $Q_{00}^{(\ell)}$, $Q_{01}^{(\ell)}$, $Q_{02}^{(\ell)}$, $Q_{10}^{(\ell)}$, $Q_{11}^{(\ell)}$ and $Q_{20}^{(\ell)}$ are

$$Q_{00}^{(\ell)} = \frac{2^{3-\ell}\pi}{E}\int_0^\infty L \sin^2 \chi_{\ell 0}\Big|_{\lambda=0}\, d\chi \tag{4.2-5}$$

$$Q_{01}^{(1)} = \frac{4\pi}{E}\left[\int_0^\infty dL \left[-\frac{1}{12} L \left(\chi'_{10}\Big|_{\lambda=0}\right)^2 \cos 2\chi_{10}\Big|_{\lambda=0} + \left(L\psi_{10}\Big|_{\lambda=0} + \frac{1}{12}\chi'_{10}\Big|_{\lambda=0}\right)\sin 2\chi_{10}\Big|_{\lambda=0}\right] + \frac{1}{24}\right] \tag{4.2-6}$$

$$Q_{01}^{(2)} = \frac{2\pi}{E}\int_0^\infty dL \left[L\psi_{20}\Big|_{\lambda=0}\sin 2\chi_{20}\Big|_{\lambda=0} - \frac{1}{3}\left(\chi'_{20}\Big|_{\lambda=0}\right)^2 \cos 2\chi_{20}\Big|_{\lambda=0} - \frac{1}{4L}\sin^2 \chi_{20}\Big|_{\lambda=0}\right] \tag{4.2-7}$$

$$Q_{02}^{(1)} = \frac{4\pi}{E}\left[\int_0^\infty dL\left[\left[\frac{L}{360}\left(\chi_{10}''|_{\lambda=0}\right)^2 + \frac{1}{6}L\chi_{10}''|_{\lambda=0}\psi_{10}|_{\lambda=0} + L\psi_{10}^2|_{\lambda=0} + \frac{1}{720}L\left(\chi_{10}'|_{\lambda=0}\right)^4 + \frac{1}{6}\chi_{10}'|_{\lambda=0}\psi_{10}|_{\lambda=0}\right]\cos 2\chi_{10}|_{\lambda=0} + \left[\frac{1}{360}\left(\chi_{10}'|_{\lambda=0}\right)^3 + L\psi_{10}|_{\lambda=0} - \frac{L}{6}\left(\chi_{10}'|_{\lambda=0}\right)^2\psi_{10}|_{\lambda=0}\right]\sin 2\chi_{10}|_{\lambda=0}\right] - \frac{7}{960}\left(\chi_{10}'(0)|_{\lambda=0}\right)^2\right] \quad (4.2\text{-}8)$$

$$Q_{02}^{(2)} = \frac{2\pi}{E}\left[\int_0^\infty dL\left[\left[\frac{2}{45}L\left(\chi_{20}''|_{\lambda=0}\right)^2 + \frac{1}{45}L\left(\chi_{20}'|_{\lambda=0}\right)^4 + \frac{2L^2}{3}\chi_{20}'|_{\lambda=0}\psi_{20}|_{\lambda=0} + L\psi_{20}^2|_{\lambda=0} + \frac{2}{3}L\chi_{20}''|_{\lambda=0}\psi_{20}|_{\lambda=0}\right]\cos 2\chi_{20}|_{\lambda=0} + \left[\frac{2}{45}\left(\chi_{20}'|_{\lambda=0}\right)^3 - \frac{2}{3}L\left(\chi_{20}'|_{\lambda=0}\right)^2\psi_{20}|_{\lambda=0} + L\varphi_{20}|_{\lambda=0} - \frac{1}{24L}\chi_{20}''|_{\lambda=0} - \frac{1}{4L}\psi_{20}|_{\lambda=0}\right]\sin 2\chi_{20}|_{\lambda=0}\right] + \frac{119}{960}\left(\chi_{20}'(0)|_{\lambda=0}\right)\right] \quad (4.2\text{-}9)$$

$$Q_{10}^{(1)} = \frac{2^{3-l}\pi}{E}\int_0^\infty L\left.\frac{\partial\chi_{20}}{\partial\lambda}\right|_{\lambda=0}\sin 2\chi_{20}|_{\lambda=0}\,dL \quad (4.2\text{-}10)$$

$$Q_{11}^{(1)} = \frac{4\pi}{E}\int_0^\infty dL\left[\left[-\frac{1}{6}\chi_{10}'|_{\lambda=0}\left.\frac{\partial\chi_{10}'}{\partial\lambda}\right|_{\lambda=0} + \frac{1}{6}\chi_{10}'|_{\lambda=0}\left.\frac{\partial\chi_{10}}{\partial\lambda}\right|_{\lambda=0} + 2L\psi_{10}|_{\lambda=0}\left.\frac{\partial\chi_{10}}{\partial\lambda}\right|_{\lambda=0}\right]\cos 2\chi_{10}|_{\lambda=0} + \left[L\left.\frac{\partial\psi_{10}}{\partial\lambda}\right|_{\lambda=0} + \frac{1}{12}\left.\frac{\partial\chi_{10}'}{\partial\lambda}\right|_{\lambda=0} + \frac{1}{6}L\left(\chi_{10}'|_{\lambda=0}\right)^2\left.\frac{\partial\chi_{10}}{\partial\lambda}\right|_{\lambda=0}\right]\sin 2\chi_{10}|_{\lambda=0}\right] \quad (4.2\text{-}10)$$

$$\Phi_{11}^{(2)} = \frac{2\pi}{E}\int_0^\infty dL \left[\begin{bmatrix} \frac{2}{3} L \left(\chi'_{20}|_{\lambda=0}\right)^2 \frac{\partial \chi_{20}}{\partial \lambda}\Big|_{\lambda=0} \\ + L \frac{\partial \psi_{20}}{\partial \lambda}\Big|_{\lambda=0} - \frac{1}{4L} \frac{\partial \chi_{20}}{\partial \lambda}\Big|_{\lambda=0} \end{bmatrix} \sin 2\chi_{20}|_{\lambda=0} + \begin{bmatrix} 2L \psi_{20}|_{\lambda=0} \frac{\partial \chi_{20}}{\partial \lambda}\Big|_{\lambda=0} \\ -\frac{2}{3} L \chi'_{20}|_{\lambda=0} \frac{\partial \chi'_{20}}{\partial \lambda}\Big|_{\lambda=0} \end{bmatrix} \cos 2\chi_{20}|_{\lambda=0} \right] \tag{4.2-12}$$

$$\Phi_{20}^{(\ell)} = \frac{2^{3-\ell}\pi}{E}\int_0^\infty \left[\frac{\partial^2 \chi_{\ell 0}}{\partial \lambda^2}\Big|_{\lambda=0} \sin 2\chi_{\ell 0}|_{\lambda=0} + 2\left(\frac{\partial \chi_{\ell 0}}{\partial \lambda}\Big|_{\lambda=0}\right)^2 \cos 2\chi_{\ell 0}|_{\lambda=0} \right] dL \tag{4.2-13}$$

In deriving these expressions the derivatives with respect to λ of χ_{n0}, χ'_{n0}, and ψ_{n0} are introduced. Explicitly these functions are

$$\frac{1}{n}\frac{\partial \chi_{n0}}{\partial \lambda} = \sigma^6 \epsilon L \int d\tau \, (E-\phi)^{-\frac{1}{2}} \left[\frac{32}{\tau^9 \phi'} + \frac{4\phi''}{\tau^8 \phi'^2} \right] \tag{4.2-14}$$

$$\frac{1}{n}\frac{\partial^2 \chi_{n0}}{\partial \lambda^2} = \sigma^{12}\epsilon^2 4L \int d\tau \, (E-\phi)^{-\frac{1}{2}} \left[-\frac{840}{\tau^{16}\phi'^2} - \frac{168\phi''^2}{\tau^{15}\phi'^3} + \frac{4\phi'''}{\tau^{14}\phi'^3} - \frac{12\phi''^2}{\tau^{14}\phi'^4} \right] \tag{4.2-15}$$

$$\frac{1}{n}\frac{\partial \chi'_{n0}}{\partial \lambda} = \sigma^6 \epsilon \int d\tau \, (E-\phi)^{-\frac{1}{2}} \left[\begin{bmatrix} \frac{32}{\tau^9 \phi'} + \frac{4\phi''}{\tau^8 \phi'^2} + \frac{880L^2}{\tau^{12}\phi'^2} \\ + \frac{240L^2\phi''}{\tau^{11}\phi'^3} - \frac{8L^2\phi'''}{\tau^{10}\phi'^3} + \frac{24L^2\phi''^2}{\tau^{10}\phi'^4} \end{bmatrix} \right] \tag{4.2-16}$$

$$\frac{1}{n}\frac{\partial \psi_{n0}}{\partial \lambda} = 48\sigma^6 \epsilon L \int d\tau \, (E-\phi)^{-\frac{1}{2}} \times \tag{4.2-17}$$

$$\times \left[\begin{bmatrix} -\frac{5610}{\tau^{12}\phi'^2} - \frac{2250\phi''}{\tau^{11}\phi'^3} - \frac{585\phi''^2}{\tau^{10}\phi'^4} - \frac{120\phi''^3}{\tau^9\phi'^5} + \frac{267\phi'''}{\tau^{10}\phi'^3} + \frac{128\phi''\phi'''}{\tau^9\phi'^4} \\ + \frac{25\phi''^2\phi'''}{\tau^8\phi'^5} - \frac{7\phi''\phi^{(iv)}}{\tau^8\phi'^4} - \frac{4\phi'''^2}{\tau^8\phi'^4} - \frac{24\phi^{(iv)}}{\tau^9\phi'^3} - \frac{15\phi''^4}{\tau^8\phi'^6} + \frac{\phi^{(v)}}{\tau^8\phi'^3} \end{bmatrix} \right]$$

In dealing with the potential

$$\varphi = 4\epsilon \left(\frac{\sigma}{r}\right)^{12} \tag{4.2-18}$$

it is advantageous to make a change in variable to dimensionless quantities defined by

$$y = \frac{L}{\sqrt{E}\, r} \qquad y_0 = \frac{L}{\sqrt{E}} \left(\frac{E}{48\epsilon\sigma^{12}}\right)^{\frac{1}{12}} \tag{4.2-19}$$

In terms of these quantities it is possible to write Eqns (4.2-5) through (4.2-13) in the form

$$Q_{00}^{(\ell)} = \left(\frac{48\epsilon}{E}\right)^{\frac{1}{6}} A_0^{(\ell)} \tag{4.2-20}$$

$$Q_{01}^{(\ell)} = \left(\frac{\epsilon}{E}\right) B_0^{(\ell)} \tag{4.2-21}$$

$$Q_{02}^{(\ell)} = \left(\frac{E}{48\epsilon}\right)^{\frac{1}{6}} C_0^{(\ell)} \tag{4.2-22}$$

$$Q_{10}^{(\ell)} = \left(\frac{\epsilon}{E}\right)\left(\frac{E}{48\epsilon}\right)^{\frac{1}{3}} A_1^{(\ell)} \tag{4.2-23}$$

$$Q_{11}^{(\ell)} = \left(\frac{\epsilon}{E}\right)^2 \left(\frac{E}{48\epsilon}\right)^{\frac{1}{2}} B_1^{(\ell)} \qquad (4.2\text{-}24)$$

$$Q_{20}^{(\ell)} = \left(\frac{\epsilon}{E}\right)^2 \left(\frac{E}{48\epsilon}\right)^{\frac{5}{6}} A_2^{(\ell)} \qquad (4.2\text{-}25)$$

where $A_0^{(\ell)}$, $B_0^{(\ell)}$, $C_0^{(\ell)}$, $A_1^{(\ell)}$, $B_1^{(\ell)}$, and $A_2^{(\ell)}$ are integrals dependent only on the exponent in the potential and the numerical coefficient of the potential (which in this case are 12 and 4 respectively). This change of variables is advantageous because it removes the energy entirely from the integrals, which is possible for these one constant potentials. This point is discussed further in Chapter V.

The integrals $B_0^{(\ell)}$, and $A_0^{(\ell)}$ have been recalculated by the author as a means of checking the numerical method against previous calculations of these quantities. Further, the integrals $C_0^{(1)}$, $C_0^{(2)}$, $A_1^{(1)}$, $A_1^{(2)}$, $B_1^{(1)}$, $B_1^{(2)}$, $A_2^{(1)}$, and $A_2^{(2)}$ have been evaluated and the results are discussed in Chapter VI.

3. The Omega Integrals

With these expressions for the $Q^{(\ell)}$ a similar series for the $\Omega^{(\ell,s)}$ integrals can be obtained, as was discussed in Chapter II. Since the energy dependence of the $Q^{(\ell)}$ is explicit,

it is possible to evaluate the $\Omega^{(\ell,s)}$ integrals exactly in terms of the gamma functions and the numerical constants introduced above. As an example of this, the integral $\Omega_{00}^{(\ell,s)}$ is evaluated in detail.

Equation (4.2-20) is substituted into Eqn. (2.3-1) to give

$$\Omega_{00}^{(\ell,s)}(T) = \frac{1}{2} A_0^{(\ell)} \sqrt{\frac{\kappa T}{2\pi\mu}} \frac{(48\epsilon)^{\frac{1}{6}}}{(\kappa T)^{s+2}} \int_0^\infty e^{-\frac{E}{\kappa T}} E^{-s+\frac{5}{6}} dE \qquad (4.3\text{-}1)$$

For convenience let

$$x = \frac{E}{\kappa T} \qquad (4.3\text{-}2)$$

which gives

$$\Omega_{00}^{(\ell,s)} = \frac{1}{2} A_0^{(\ell)} \sqrt{\frac{\kappa T}{2\pi\mu}} \left(\frac{48\epsilon}{\kappa T}\right)^{\frac{1}{6}} \int_0^\infty e^{-x} x^{-s+\frac{5}{6}} dx \qquad (4.3\text{-}3)$$

The integral is of the gamma function type[26] and thus $\Omega_{00}^{(\ell,s)}$ is

$$\Omega_{00}^{(\ell,s)} = \frac{1}{2} A_0^{(\ell)} \sqrt{\frac{\kappa T}{2\pi\mu}} \left(\frac{48\epsilon}{\kappa T}\right)^{\frac{1}{6}} \Gamma\left(-s+\frac{11}{6}\right) \qquad (4.3\text{-}4)$$

By similar methods we find

$$\Omega_{01}^{(\ell,s)} = \frac{1}{2} B_0^{(\ell)} \sqrt{\frac{kT}{2\pi\mu}} \frac{1}{kT} \Gamma(s+1) \qquad (4.3\text{-}5)$$

$$\Omega_{02}^{(\ell,s)} = \frac{1}{2} C_0^{(\ell)} \sqrt{\frac{kT}{2\pi\mu}} \left(\frac{1}{48\epsilon}\right)^{\frac{1}{6}} \frac{1}{(kT)^{\frac{11}{6}}} \Gamma(s+\tfrac{1}{6}) \qquad (4.3\text{-}6)$$

$$\Omega_{10}^{(\ell,s)} = \frac{1}{2} A_1^{(\ell)} \sqrt{\frac{kT}{2\pi\mu}} \left(\frac{1}{48\epsilon}\right)^{\frac{1}{3}} \frac{1}{(kT)^{\frac{2}{3}}} \Gamma(s+\tfrac{4}{3}) \qquad (4.3\text{-}7)$$

$$\Omega_{11}^{(\ell,s)} = \frac{1}{2} B_1^{(\ell)} \sqrt{\frac{kT}{2\pi\mu}} \left(\frac{1}{48\epsilon}\right)^{\frac{1}{2}} \frac{1}{(kT)^{\frac{3}{2}}} \Gamma(s+\tfrac{1}{2}) \qquad (4.3\text{-}8)$$

$$\Omega_{20}^{(\ell,s)} = \frac{1}{2} A_2^{(\ell)} \sqrt{\frac{kT}{2\pi\mu}} \left(\frac{1}{48\epsilon}\right)^{\frac{5}{6}} \frac{1}{(kT)^{\frac{7}{6}}} \Gamma(s+\tfrac{5}{6}) \qquad (4.3\text{-}9)$$

This double series shows the effect of the attractive part of the Lennard-Jones (12,6) potential on the classical value and the quantum corrections to the transport properties and their cross sections. The terms "00", "01", and "02" give the classical limit

and the first and second quantum corrections for a gas of molecules which repel each other as the inverse twelfth power of the distance between them.

The terms "10", "11", and "20", in conjunction with "00", "01", and "02", provide a check at high energies on the results using the Lennard-Jones potential. The numerical work involved in the latter calculations is much more complex. This is discussed in the next chapter.

CHAPTER V

NUMERICAL PROCEDURES

The difficulties in the numerical evaluation of the expressions obtained in Chapters II, III, and IV can be divided into two types: (1) the evaluation of the Bessel functions in Eqn. (3.5-1) and (2) the numerical integrations involved in the evaluation of the omega integrals in Chapter II and IV. The former problem is reasonably straightforward and offers no great difficulty. The latter problem, however, is complicated in that the omega integrals are really double integrals involving very nasty and ill-behaved functions. These integrals also depend on whether the potential is monotonic or has a minimum. These cases are treated separately.

1. Dimensionless quantities

Before proceeding to the numerical calculations, it is convenient to introduce several dimensionless quantities. For this purpose the intermolecular potential is taken to be of the form

$$\varphi = \epsilon F\left(\frac{r}{\sigma}\right) \tag{5.1-1}$$

where ϵ is an energy parameter (the depth of the well for potentials with a minimum) and σ is a length parameter (the point where $\varphi(r) = 0$ for potentials with a minimum). In terms of these parameters we define the following reduced quantities:

$$r^* = \frac{r}{\sigma} \qquad T^* = \frac{kT}{\epsilon}$$

$$b^* = \frac{L}{\sigma\sqrt{E}} \qquad E^* = \frac{E}{\epsilon} \tag{5.1-2}$$

$$\varphi^* = \frac{\varphi}{\epsilon} \qquad \phi^* = \varphi^* + \frac{b^{*2}E^*}{r^{*2}}$$

It is convenient to make $Q^{(\ell)}$ and $\Omega^{(\ell,s)}$ dimensionless by dividing then by their corresponding classical rigid sphere values[27]. Thus,

$$Q^{(\ell)*} = \frac{Q^{(\ell)}}{\left[1 - \frac{1}{2}\cdot\frac{1+(-1)^\ell}{1+\ell}\right]\pi\sigma^2}$$

$$\Omega^{(\ell,s)*} = \frac{\Omega^{(\ell,s)}\sqrt{\frac{2\pi u}{kT}}}{\frac{1}{2}(s+1)!\left[1 - \frac{1}{2}\cdot\frac{1+(-1)^\ell}{1+\ell}\right]\pi\sigma^2} \tag{5.1-3}$$

It is also convenient to introduce a dimensionless quantum parameter involving Planck's constant. This parameter, called the de Boer quantum parameter, is defined as

$$\Lambda^* = \frac{h}{\sigma\sqrt{2u\epsilon}} \tag{5.1-4}$$

This is the de Broglie wavelength of the relative motion of two

molecules, with relative kinetic energy ϵ , divided by the characteristic length σ . Since Λ^* is introduced only as a dimensionless parameter, it is rather unfortunate numerically that h , and not $\hbar$ was used in the definition.

With the aid of these definitions, the equations of the previous chapters may be written in dimensionless form. It is understood that although the stars may be dropped all succeeding equations are in terms of dimensionless quantities.

2. The Square Well Potential

It has not been possible to compare analytically the classical, classical limit, and quantum expressions for $Q^{(1)}$ and $Q^{(2)}$ for the square well potential. The complicated nature of the expression for the phase shifts, Eqn. (3.5-1) apparently makes this impossible. As a result of this, it is necessary to resort to a numerical comparison. The classical and classical limit expressions for $Q^{(1)}$ and $Q^{(2)}$, Eqns. (3.3-17),(3.3-20), (3.4-7), and (3.4-8), are very easy to evaluate numerically since the energy is related to η by Eqn. (3.3-3). The quantum calculation of $Q^{(1)}$ and $Q^{(2)}$ is more complicated because it is necessary to first evaluate the phase shifts, Eqn. (3.5-1), for many values of ℓ and then use these phase shifts in Eqns. (2.1-1) and (2.1-2). The calculation of the phase shifts depends on the calculation of the Bessel functions, which were calculated by the method described by Olver.[28]

The calculation of $\Omega^{(1)}$ and $\Omega^{(2)}$ starts at $\ell = 0$ and proceeds to $\ell_{max} + 2$, where ℓ_{max} is the first integer greater than

$$\ell_{max} = \frac{2\pi\sqrt{1+E^*}}{\Lambda^*} - \frac{1}{2} \qquad (5.2\text{-}1)$$

This value of ℓ corresponds to the largest value of b for which the energy of collision is in the collision region (see Fig. 3-2b of Chapter III). For greater values of b (and thus ℓ) the particles do not interact and so the phase shift goes to zero.

In this manner it is possible to obtain $\Omega^{(1)}$ and $\Omega^{(2)}$ as numerical functions of the energy for the classical, classical limit, and quantum cases. These three quantities are compared in Chapter VI.

3. Monotonic Potentials

The calculation of the omega integrals for monotonic potentials, while somewhat involved, is a reasonably straightforward application of well-known numerical procedures. The omega integrals are triple integrals over the trajectory of the particles, the impact parameter, and the energy. The last integration, as was demonstrated in Chapter IV, can be done analytically.

The integration over the trajectory (actually over one-half of the trajectory) to get the functions in Eqns. (2.1-7) through (2.1-11) and (4.2-14) through (4.2-17) has the limits (r_1, ∞) where r_1 is the positive real root of the equation

$$E^* - \phi^* = 0 \tag{5.3-1}$$

Explicitly this equation is

$$r^{*12} - b^{*2} r^{*10} - \frac{4}{E^*} = 0 \tag{5.3-2}$$

The Newton-Raphson method[29] was used to find the root.

The integrands of the functions in Eqns. (2.1-7) through (2.1-11) and (4.2-14) through (4.2-17) are such that they have a pole of order one-half at the lower limit of the integration. The numerical integration in this case is most easily done using the Gauss-Mehler method.[30]

The integration over b , or since there is a change of integration for this potential, over y_o , to obtain the integrals was carried out using the Gauss-Legendre method.[31] The range of integration is $(0, \infty)$. However, since the integrand becomes small long before the upper limit is reached, it is only necessary to integrate to about $y_o = 2$.

It was shown in Chapter IV that the integration over the energy can be carried out analytically in terms of gamma functions. This is possible because potentials of the type

$$\varphi = \frac{d}{r^\delta} \tag{5.3-3}$$

are really one constant (d) potentials and it is always possible

to make a change of variable (as is done in Chapter IV) that factors the energy out of the $Q^{(l)}$ integrals. In general, this substitution is

$$y_o = \frac{L}{\sqrt{E}} \left(\frac{E}{\delta d} \right)^{\frac{1}{\delta}} \qquad (5.3\text{-}4)$$

For two constant potentials, such as the Lennard-Jones potential, this is not possible and the omega integrals must also be carried out numerically. This point is discussed in the next section.

4. Potentials with a Minimum

While the methods of integration over the trajectory and the impact parameter remain the same as for monotonic potentials, their application is quite different for potentials with a minimum. Moreover, the omega integrals must be handled in an entirely different manner because the energy dependence of the $Q^{(l)}$ integrals does not factor out.

A typical potential with a minimum, and the one chosen for this work, is the Lennard-Jones (12,6) potential defined as

$$\varphi = 4\epsilon \left[\left(\frac{\sigma}{r} \right)^{12} - \left(\frac{\sigma}{r} \right)^{6} \right] \qquad (5.4\text{-}1)$$

where ϵ is the depth of the minimum and σ is the value of r when $\varphi = 0$. The reduced effective potential

$$\phi^* = 4\left(\frac{1}{r^{*12}} - \frac{1}{r^{*6}}\right) + \frac{b^{*2}E^*}{r^{*2}} \qquad (5.4\text{-}2)$$

has both a maximum and a minimum for values of the product $b^{*2}E^*$ below a critical value $\frac{36}{25}\sqrt[3]{5}$. For values above this critical value the effective potential decreases monotonically. The effective potential is plotted for various values of $b^{*2}E^*$ in Figures 5.4a, b, c, and d .

The fact that the effective potential has a maximum and a minimum for some values of $b^{*2}E^*$ means, of course, that its derivative is zero at these points. It becomes necessary, then, in deriving the expressions for $\eta_\ell^{(2)}$ and $\eta_\ell^{(3)}$ (and thus the five basic functions (Eqns. (2.1-6))to integrate by parts around these points. To get a clearer picture of exactly what the final range of integration is, three cases are considered. These are shown graphically in Fig. 5.4a, b, c, and d. These plots show the effective potential and the horizontal line representing the energy of the particular collision. The intersections of the curve and the straight line are the turning points (lower limit of integration) on the trajectories.

In Case I the energy and the impact parameter are such that $\frac{\partial \phi^*}{\partial r^*}$ is zero at two points on the trajectory. The integration by parts, Eqn. (57) of reference 14, employed in the derivation of the phase shift series is not valid at these points. However, if a

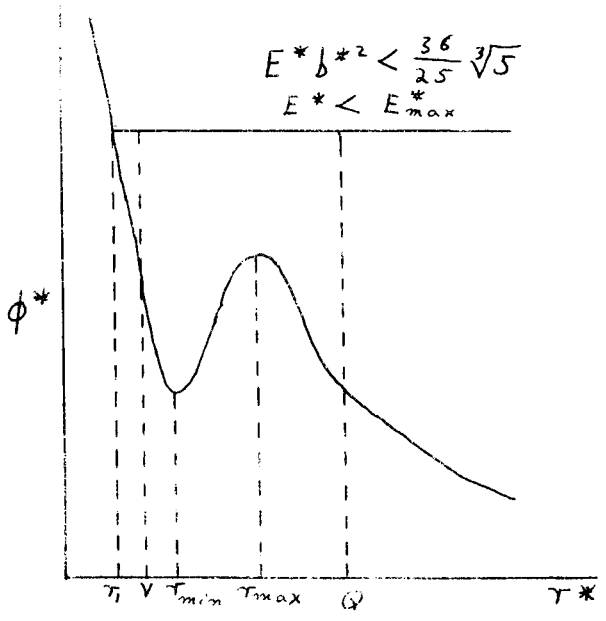

Case I

Figure 5 - 4a

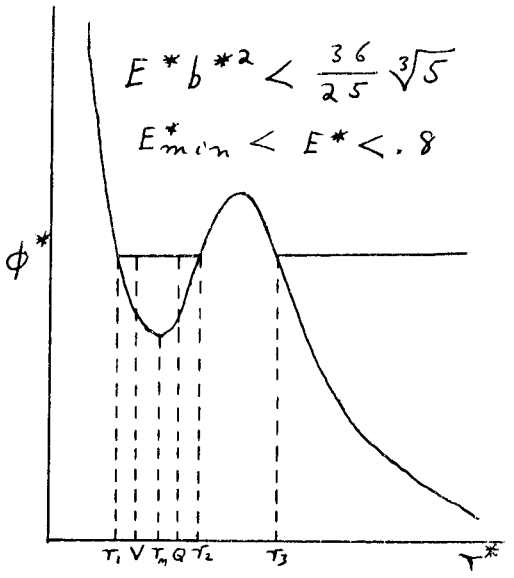

Case II

Figure 5 - 4b

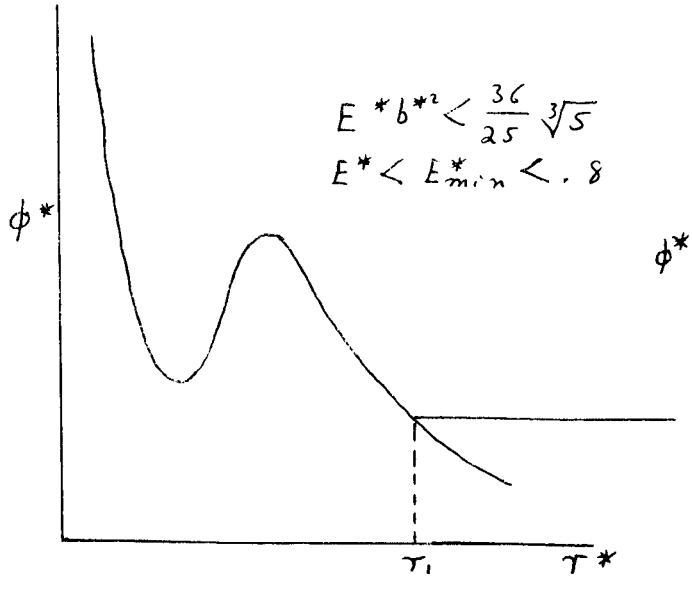

Case III

Figure 5 - 4c

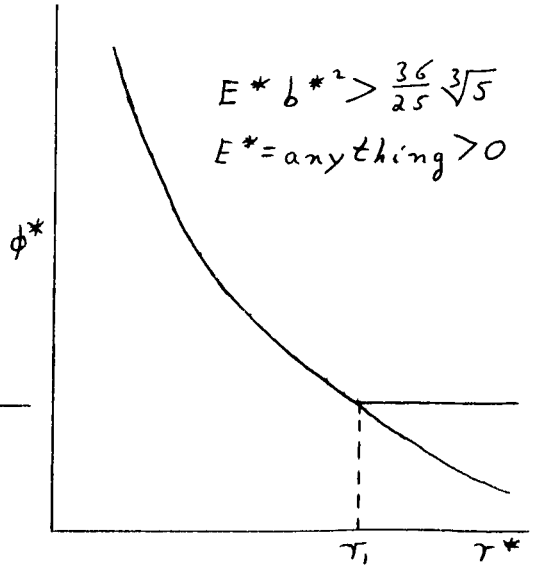

Figure 5 - 4d

point V is chosen between r_1 and r_{min}, and a point Q is chosen beyond r_3, it is possible to integrate by parts between r_1 and V and Q and infinity. Between V and Q nothing more can be done to simplify the integrals.

Case II is handled in exactly the same manner; V is chosen between r_1 and r_{min}, and Q is chosen between r_{min} and r_2.

Case III is simple because nowhere on the trajectory does $\frac{\partial \phi^*}{\partial r^*}$ become zero. Thus, the integration by parts is used to simplify the expressions.

In the derivation of the five basic functions Eqns. (2.1-7) through (2.1-11), it is necessary to consider these three cases also.

While the choice of V and Q is immaterial, subject to the above limitations, they are defined for convenience as

Case I: $$V = \frac{1}{2}(r_1 + r_{min}) \qquad Q = r_{max} + 1$$

Case II: $$V = \frac{1}{2}(r_1 + r_{min}) \qquad Q = \frac{1}{2}(r_{min} + r_2)$$

(5.4-3)

The integration is done using the Meller-Gauss method, just as for the monotonic potential. In the integrations from V to Q the Mehler-Gauss is also used.

The integration over the impact parameter is also complicated by the existence of the maximum and minimum in the effective potential. For energies above $E^* = 2$ the integrands become very

small rapidly for increasing b^*. Thus, the upper limit of integration is taken to be $b^*=3$ and not $b^*=\infty$. For energies in the range $.8<E^*\leq 2$ the integration over b^* is broken into the regions (0, 1.8) and (1.8,4). Finally, for $E^*\leq .8$ the integration over b^* is broken into three parts: from $b^*=0$ to a value of b^* such that the maximum of ϕ^* is just tangent to the energy line, from the latter point to the value of b^* such that the minimum of ϕ^* is just tangent to the energy line, and from this point to $b^*=4$. In all of these cases the Gauss-Legendre method of numerical integration is used.

Since the $Q^{(\ell)*}$ are of interest in themselves, a change of variables is made in the omega integrals so that the $Q^{(\ell)*}$ are calculated as a function of $\ln E^*$. This was advantageous because the $Q^{(\ell)*}$ change slowly for large E^*. The change of variables is $z=\ln E^*$ and the omega integrals are

$$\Omega^{(\ell,s)*}=\left[(s+1)!\,T^{*s+2}\right]^{-1}\int_{-\infty}^{\infty}Q^{(\ell)*}\exp\left[(s+2)z^*-\frac{1}{T^*}\exp z\right]dz \qquad (5.4\text{-}4)$$

The integrals, for various ℓ and s are calculated using Hardy's rule.[32] The highest temperature for which these integrals may be accurately calculated depends on the range of energies used in the calculation of the $Q^{(\ell)*}$ integrals. In order to estimate the error due to truncating the range of E^*, an integration can be done (for all of the temperatures considered) with all of the $Q^{(\ell)*}$ set

equal to unity. Since the integral of the full range is unity (with $g^{(0)*} = 1$), the deviation from unity serves as a good estimate of the truncation error.

All of the numerical work was carried out on the CDC 1604 computer at the University of Wisconsin Numerical Analysis Laboratory.

CHAPTER VI

DISCUSSION OF RESULTS

In this chapter the results of the numerical evaluation of the $Q^{(\ell)*}$ and the $\Omega^{(\ell,s)*}$ are presented for the three potentials studied in this thesis. For the square well potential the classical and classical limit expressions for the $Q^{(\ell)*}$ are compared. A comparison is also made of the high reduced energy and temperature values of the $Q^{(\ell)*}$ and the $\Omega^{(\ell,s)*}$ for the (12-6) potential with the results of the perturbation expansion. Both of these latter developments are explored.

Tables of $Q^{(1)*}$ and $Q^{(2)*}$ as functions of the reduced energy are presented along with the $\Omega^{(\ell,s)*}$ for (ℓ,s) equal to (1,1), (1,2), (1,3), (2,2), (2,3) and (2,4) as functions of the reduced temperature for the (12-6) potential. Various plots are also presented.

1. The Square Well Potential

Figure (6.1-2) shows for the square well potential the classical, the classical limit, and the quantum $Q^{(1)*}$ for $\Lambda^* = 1$ (the plots for $Q^{(2)*}$ are of the same form and so only $Q^{(1)*}$ is presented in this comparison). The limiting forms, $Q_{CL}^{(1)*}$ and $Q_{CL}^{(1)*}$, discussed in Chapter III, are also illustrated in this plot. The quantum $Q^{(1)*}$ is smooth down to a reduced energy of about .95 and then begins to oscillate, finally becoming very large (probably

going to infinity) at low reduced energy.

Figure (6.1-3) again shows $Q_{el}^{(1)*}$ and $Q_{CL}^{(1)*}$ along with $Q_{qu}^{(1)*}$ for $\Lambda^* = .5$. The quantum curve has many more oscillations for this value of Λ^* than for $\Lambda^* = 1$. The oscillations begin higher on the reduced energy scale, are much sharper, and the peaks are not as high. The general trend is that $Q_{qu}^{(1)*}$ is lower for $\Lambda^* = .5$ than for $\Lambda^* = 1$.

Finally, Fig. (6.1-4) shows the same quantities for $\Lambda^* = .1$. At this low value of Λ^* the oscillations appear to be almost wiped out. Again the general trend is that the quantum curve is lower, becoming large at an extremely low reduced energy. Because of computer time requirements it was impossible to go to lower values of Λ^*.

Figure (6.1-5) is a plot of the partial sums (see Eqn. (2.1-1)) of $Q_{qu}^{(1)*}$ (for $E^* = 1.8$) versus $(\ell + \frac{1}{2})\Lambda^*$. From Eqn. (5.2-1) we see that

$$(\ell + \tfrac{1}{2})\Lambda^* = 2\pi\sqrt{1 + E^*} \qquad (6.1\text{-}1)$$

and thus $(\ell + \frac{1}{2})\Lambda^*$ is a constant for fixed energy. Thus, the same scale on the abscissa can be used for all values of Λ^*. The partial sums all become greater than the classical limit before the three turning point region is reached. The contribution from the

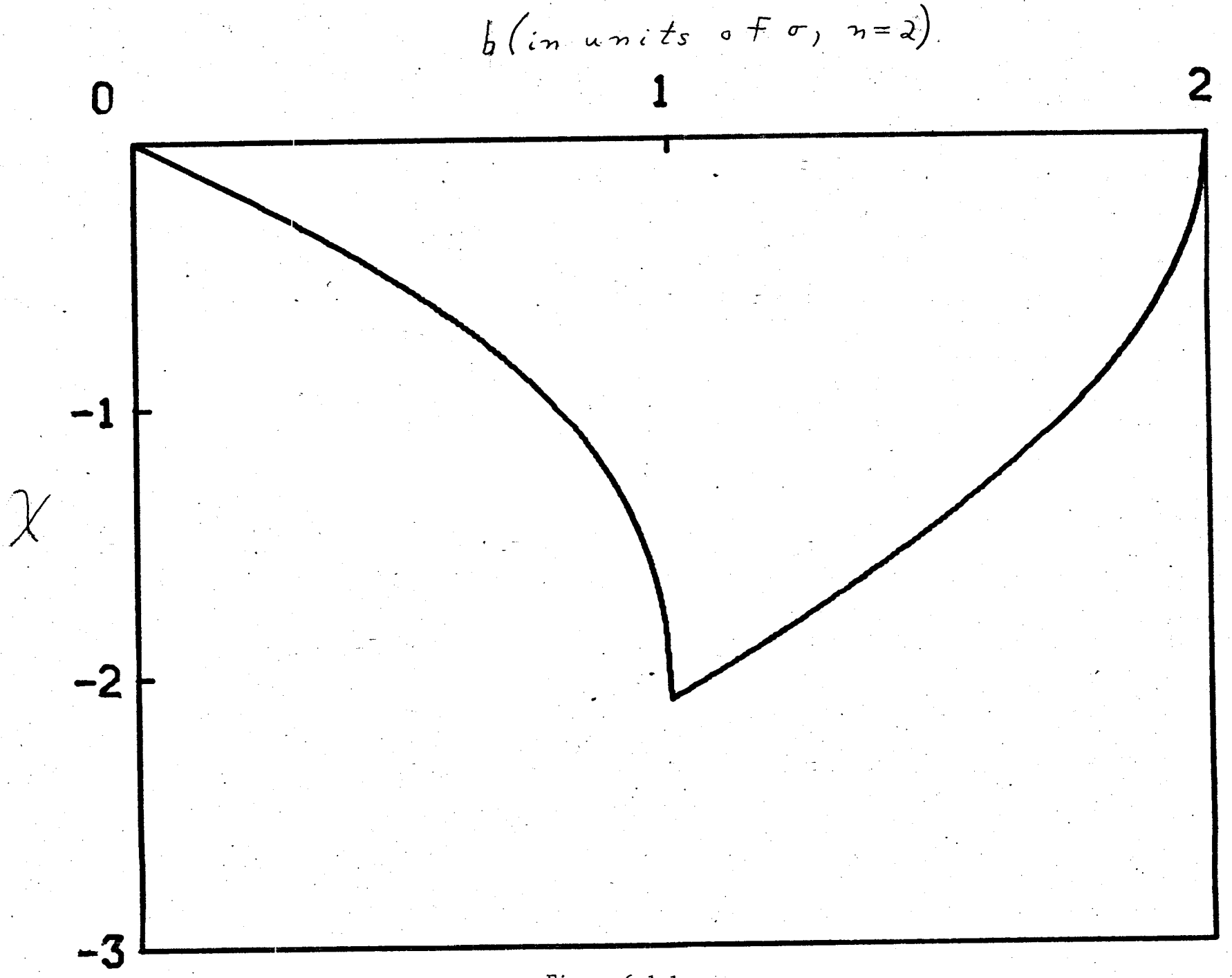

Figure 6.1-1

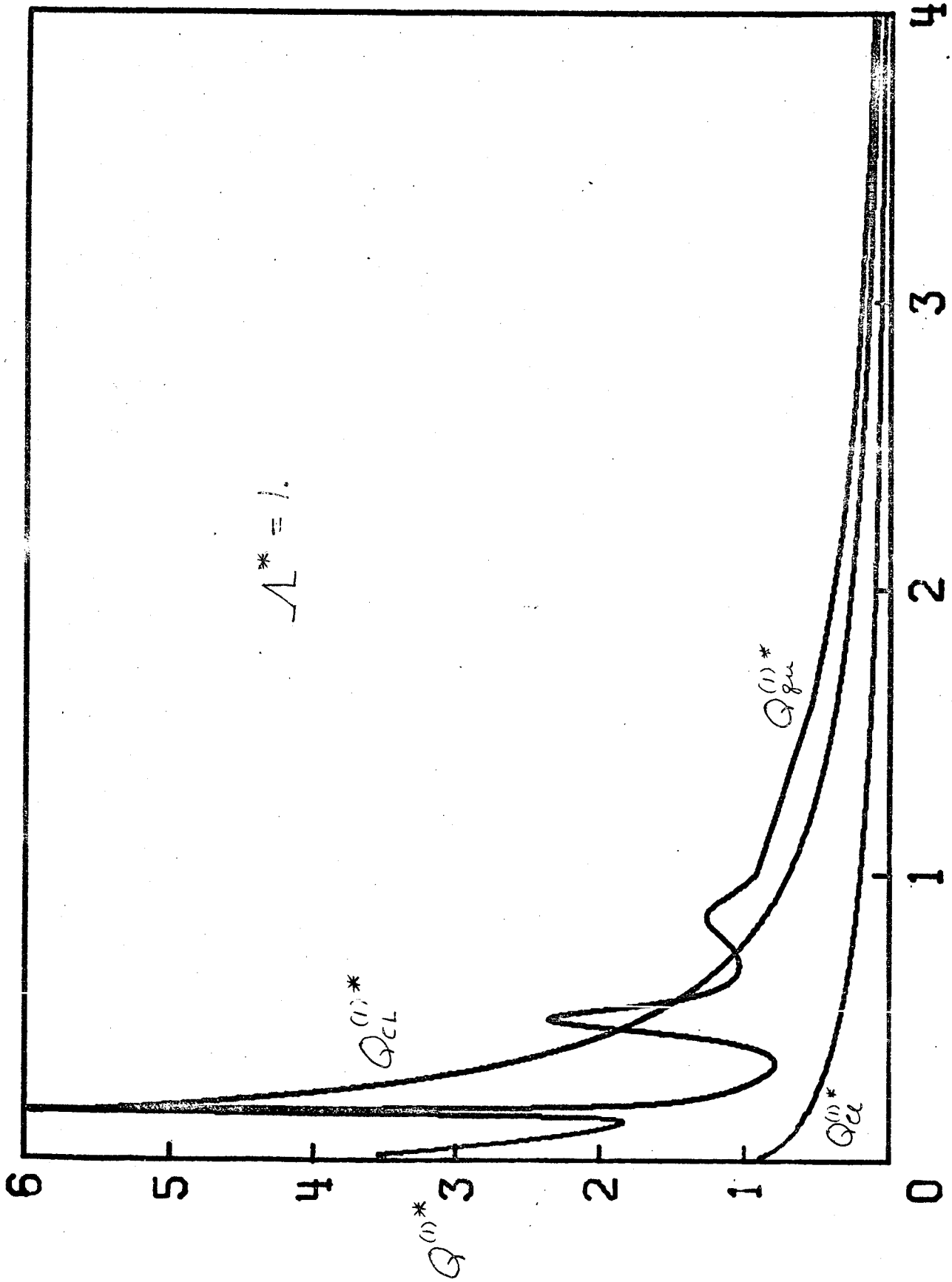

Figure 6.1-2

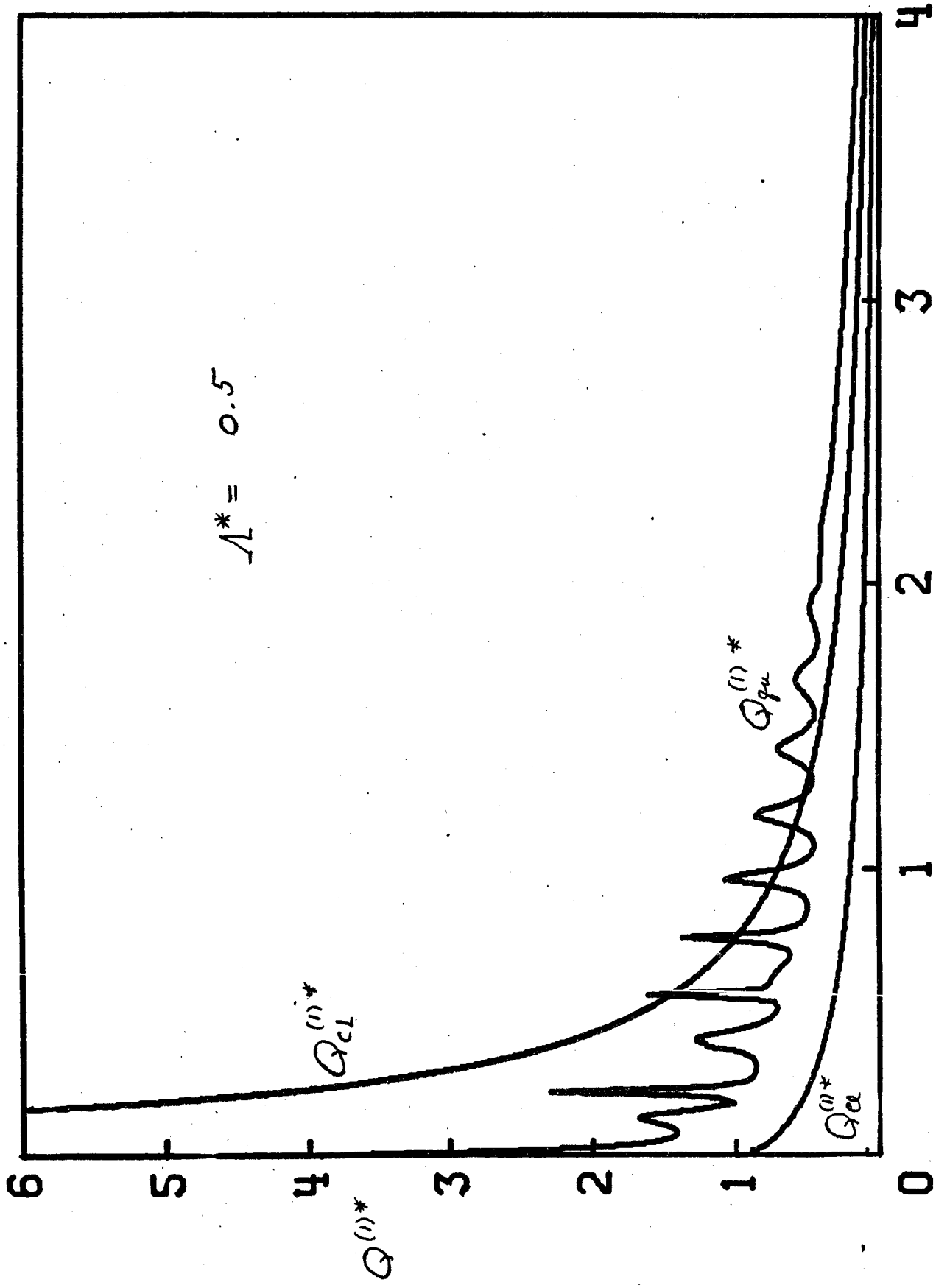

Figure 6.1-2

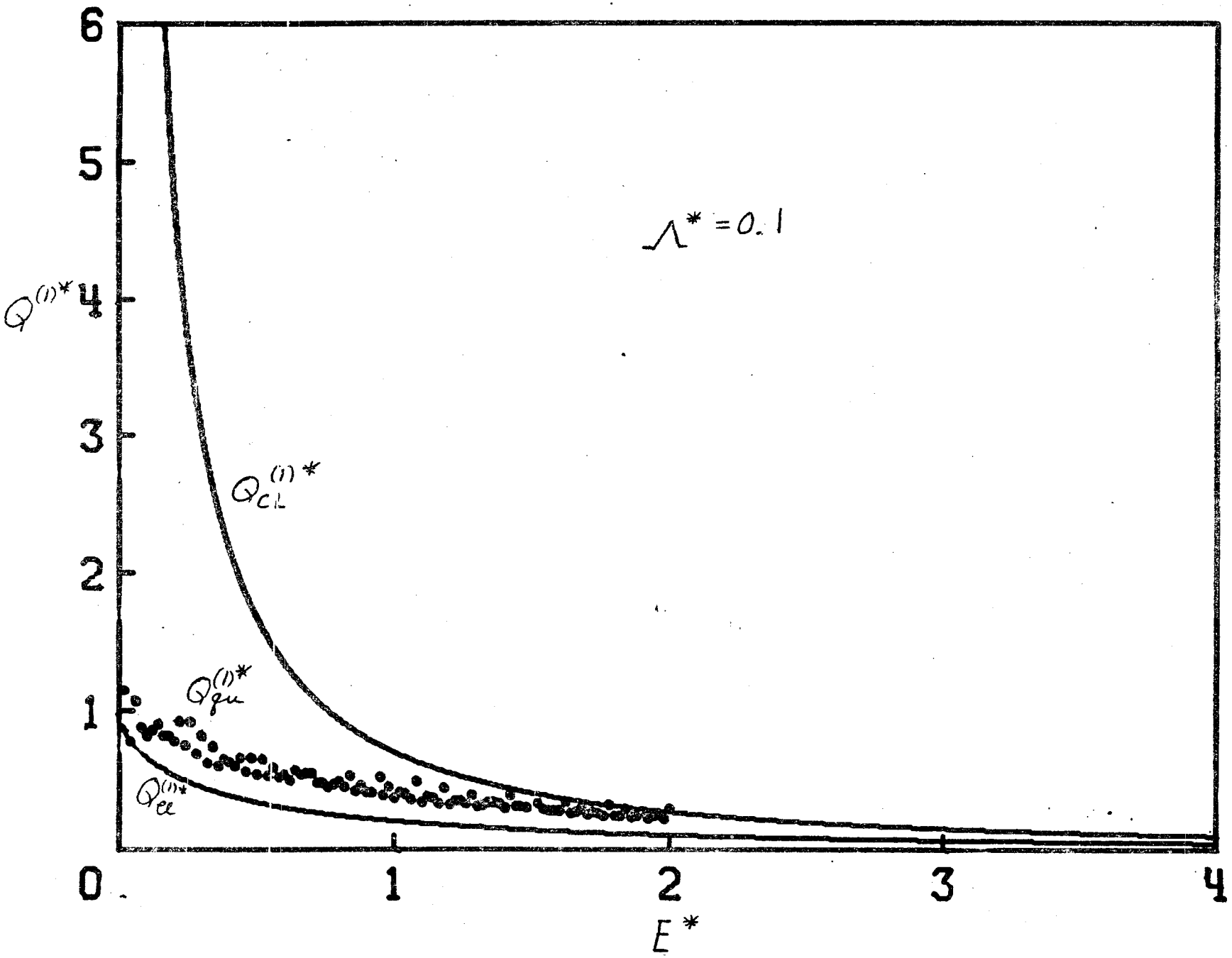
6
5
4
3
2
1
0
1
2
3
4
$Q^{(1)*}$
E^*
$\Lambda^* = 0.1$
$Q_{cL}^{(1)*}$
$Q_{qu}^{(1)*}$
$Q_{ee}^{(1)*}$

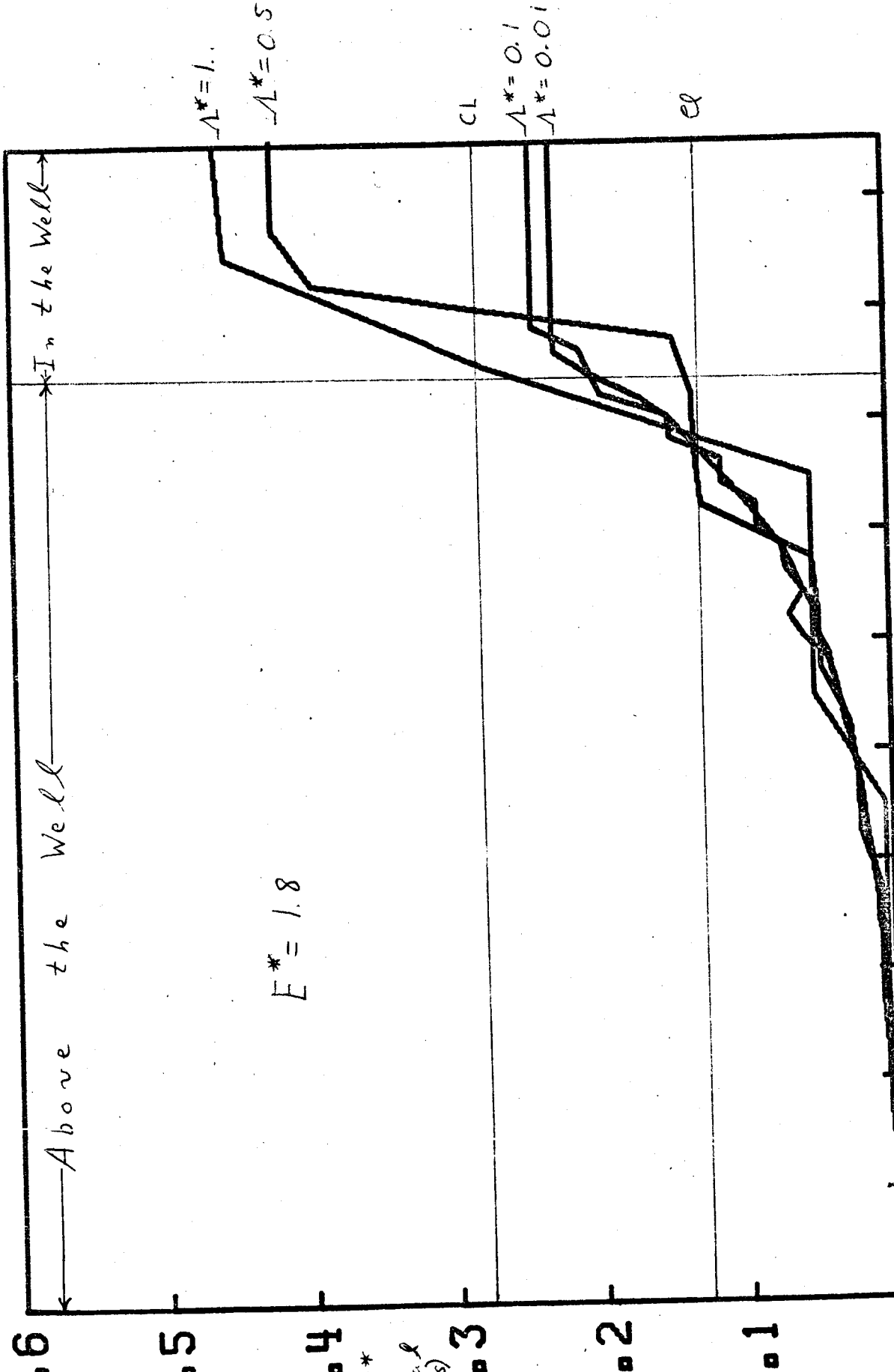
$\Lambda^* = 1.$
$\Lambda^* = 0.5$
CL
$\Lambda^* = 0.1$
$\Lambda^* = 0.01$
eq
Above the Well
In the Well
$E^* = 1.8$
$Q^{(1)*}$ (partial sums)
$(\ell + \frac{1}{2})\Lambda^*$
0 1 2 3 4 5 6 7 8 9 10
.1 .2 .3 .4 .5 .6

Figure 6.1-5

three turning point region is very small for small values of Λ^*. As a matter of fact, most of the contribution to the $Q_{qu}^{(1)*}$ comes from a region near the top of the well. This may be a diffraction effect caused by the sharpness of well.

The results presented here are somewhat inconclusive. At high reduced energies the quantum, classical limit, and classical curves appear to approach a common limit, with the quantum curve approaching from the same side as the classical limit. At lower reduced energies and lower values of Λ^*, however, the quantum curve moves in between the classical limit and the classical curves.

While this potential gives nice integrals in the classical limit, it would be difficult to consider the higher terms in the series because the potential does not possess continuous derivatives. It may be, then, that this comparison is not valid because the series using this potential may not have a classical limit (that is, the semiclassical development may not be valid for this potential because of the discontinuous derivatives).

This view is supported by calculations[34] for the Lennard-Jones (12-6) potential. For this differentiable potential the classical limit of the phase shift does agree with the quantum calculations in the three turning point region.

With this confidence in the validity of the classical limit we proceed to a more realistic potential.

2. Purely Repulsive Potentials and the Perturbation Expansion

Equation (4.2-3) gives $Q^{(2)*}$ as a double series in h^2 and λ. Since λ is simply an ordering parameter it is set equal to unity at this point. Also, for dimensional reasons h is replaced by Λ^*. In terms of the calculated coefficients $Q^{(1)*}$ and $Q^{(2)*}$ are

$$Q^{(1)*} = 1.3180\, E^{*-\frac{1}{6}} + 3.4609 \times 10^{-3} E^{*-1}\Lambda^{*2} + 4.7294 \times 10^{-3} E^{*-\frac{11}{6}}\Lambda^{*4} + \ldots$$

$$-4.3068 \times 10^{-1} E^{*-\frac{2}{3}} - 6.3468 \times 10^{-2} E^{*-\frac{3}{2}}\Lambda^{*2} + \ldots$$

$$+8.9255 \times 10^{-1} E^{*-\frac{7}{6}} + \ldots \qquad (6.2\text{-}1)$$

$$+ \ldots.$$

$$Q^{(2)*} = 1.5938\, E^{*-\frac{1}{6}} + 3.9115 \times 10^{-2} E^{*-1}\Lambda^{*2} + 9.8558 \times 10^{-3} E^{*-\frac{11}{6}}\Lambda^{*4} + \ldots$$

$$-8.6472 \times 10^{-1} E^{*-\frac{2}{3}} - 1.4923 \times 10^{-1} E^{*-\frac{3}{2}}\Lambda^{*2} + \ldots$$

$$+1.6120\, E^{*-\frac{7}{6}} + \ldots$$

$$+ \ldots$$

(6.2-2)

The terms in these expressions are written in the same order as Eqn. (4.2-3).

Some general features are common to both of these expansions. The first "row" of numbers contains only positive numbers (at least through terms in Λ^{*4}, the second "row" numbers are all negative, and the third row has one positive number. Since this occurs in both cases it leads to the conclusion that this may be a general rule. A study of the results for the Lennard-Jones (12-6) potential at high reduced energy supports this conclusion. The asymtotic nature of the expansions is also apparent, moreso in $Q^{(1)*}$ than $Q^{(2)*}$ because of the much greater coefficients.

At high reduced energies these series expressions should approach the corresponding classical limit and second and fourth quantum corrections for the Lennard-Jones (12-6) potential. At a reduced energy of 630.96 the comparison of $Q_{CL}^{(1)*}$ is

$$Q_{CL}^{(1)*} = .45003$$

$$\frac{\partial Q_{CL}^{(1)*}}{\partial \lambda} = -.00585 \qquad (6.2\text{-}3)$$

$$\frac{\partial^2 Q_{CL}^{(1)*}}{\partial \lambda^2} = .00048$$

Sum = .44466 $\qquad Q_{CL}^{(1)*}\Big|_{L\text{-}J} = .44445$

For $Q_{CL}^{(2)*}$ the comparison is

$$Q_{CL}^{(2)*} = .54420$$

$$\frac{\partial Q_{CL}^{(2)*}}{\partial \lambda} = -.01175 \qquad (6.2\text{-}4)$$

$$\frac{\partial^2 Q_{CL}^{(2)*}}{\partial \lambda^2} = .00087$$

Sum = .53332 $\qquad Q_{CL}^{(2)*}\big|_{L\text{-}J} = .53292$

In both cases the error is in the fourth place. Both values obtained from the perturbation expansion are higher than the corresponding result for the Lennard-Jones potential. If the series in the classical limit is alternating (as is indicated by the first three terms), the fourth term would be negative and make the agreement even better. Thus, even at this high energy at least four terms in the series are needed for excellent agreement.

At the same energy the comparison for $Q_{II}^{(1)*}$ is

$$Q_{II}^{(1)*} = +5.4851 \times 10^{-6}$$

$$\frac{\partial Q_{II}^{(1)*}}{\partial \lambda} = -4.0045 \times 10^{-6} \qquad (6.2\text{-}5)$$

$$\text{Sum} = 1.4806 \times 10^{-6} \qquad Q_{II}^{(1)*}\Big|_{L\text{-}J} = 1.3351 \times 10^{-7}$$

For $Q_{II}^{(2)*}$ the comparison is

$$Q_{II}^{(2)*} = 6.1993 \times 10^{-5}$$

$$\frac{\partial Q_{II}^{(2)*}}{\partial \lambda} = -0.9416 \times 10^{-5} \qquad (6.2\text{-}6)$$

$$\text{Sum} = 5.2577 \times 10^{-6} \qquad Q_{II}^{(2)*}\Big|_{L\text{-}J} = 5.0998 \times 10^{-5}$$

These results appear somewhat surprising since for $Q_{II}^{(1)*}$ the sum of the two terms in the perturbation series gives a result greater than the result for the Lennard-Jones potential while for $Q_{II}^{(2)*}$ the opposite is true. An analysis of the behavior of the results for the Lennard-Jones potential as a function of the energy explains this seemingly anomolous behavior. Up to a reduced energy of about

44 both $Q_{II}^{(1)*}$ and $Q_{II}^{(2)*}$ are negative, but becoming less negative. At a reduced energy slightly greater than 44 $Q_{II}^{(2)*}$ becomes positive and continues to become greater. At a reduced energy of about 112 $Q_{II}^{(2)*}$ goes through a maximum and begins to decrease and approaches the perturbation result from above. The behavior of $Q_{II}^{(1)*}$ appears to be the same, but $Q_{II}^{(1)*}$ does not become positive until about 631 on the reduced energy scale. Thus, it probably does not reach a maximum until a much greater energy.

At a reduced energy of 630.96 the comparison for $Q_{IV}^{(1)*}$ is

$$Q_{IV}^{(1)*} = 3.4792 \times 10^{-8} \qquad Q_{IV}^{(1)*}\Big|_{L\text{-}J} = 4.2263 \times 10^{-7} \qquad (6.2\text{-}7)$$

For $Q_{IV}^{(2)*}$ the comparison is

$$Q_{IV}^{(2)*} = 7.2505 \times 10^{-8} \qquad Q_{IV}^{(2)*}\Big|_{L\text{-}J} = 1.0561 \times 10^{-7} \qquad (6.2\text{-}8)$$

In both cases the result for the Lennard-Jones potential is above and decreasing to the perturbation series result.

This perturbation series, like most perturbation series, probably behaves asymptotically. That is, as lower reduced energies are considered the higher terms in the series become large and overwhelm the first few terms in the series. However, for a finite

number of terms and for high enough reduced energy the finite series behaves nicely. The series for the classical limits (the first columns of Eqns. (6.2-1) and (6.2-2)) are much better behaved than the series for the quantum corrections. Likewise it appears that the series for the first quantum corrections are better than those for the second quantum corrections. From this behavior it seems that the series is asymtotic in Λ^* as well. This is to be expected since the phase shift series, which is the basis for this work, is probably asymtotic.

The perturbation series for $\Omega^{(1,1)*}$ and $\Omega^{(2,2)*}$ are roughly the same, comparatively, as that for $Q^{(1)*}$ and $Q^{(2)*}$. The results can not be expected to be as good because the omega integrals are transforms on the energy and thus have contributions from an energy range (see Eqn. (2.3-1)).

In terms of the calculated quantities the series for $\Omega^{(1,1)*}$ and $\Omega^{(2,2)*}$ are

$$\Omega^{(1,1)*} = 1.1363 T^{*-\frac{1}{6}} + 1.7304 \times 10^{-3} T^{*-1} \Lambda^{*2} + 2.1935 \times 10^{-3} T^{*-\frac{11}{6}} \Lambda^{*4}$$

$$-2.5697 \times 10^{-1} T^{*-\frac{2}{3}} - 2.8124 \times 10^{-2} T^{*-\frac{3}{2}} \Lambda^{*2} + \ldots \qquad (6.2\text{-}9)$$

$$+4.1975 \times 10^{-1} T^{*-\frac{7}{6}} + \ldots$$

$$\Omega^{(2,2)*} = 1.2978\,T^{*-\frac{1}{6}} + 1.3038 \times 10^{-2} T^{*-1} \Lambda^{*2} + 1.7778 \times 10^{-3} T^{*-\frac{11}{6}} \Lambda^{*4} + \ldots$$

$$-4.0013 \times 10^{-1} T^{*-\frac{2}{3}} - 3.3062 \times 10^{-2} T^{*-\frac{3}{2}} \Lambda^{*2} + \ldots \qquad (6.2\text{-}10)$$

$$+7.1597 \times 10^{-1} T^{*-\frac{7}{6}}$$

At a reduced temperature of 50 the comparison of $\Omega_{CL}^{(1,1)*}$ from the perturbation series with that of the Lennard-Jones potential is

$$\Omega_{CL}^{(1,1)*} = .59201$$

$$\frac{\partial \Omega^{(1,1)*}}{\partial \lambda} = -.01893 \qquad (6.2\text{-}11)$$

$$\frac{\partial^2 \Omega^{(1,1)*}}{\partial \lambda^2} = .00437$$

$$\text{Sum} = .57745 \qquad \Omega_{CL}^{(1,1)*}\Big|_{L\text{-}J} = .57582$$

For $\Omega_{CL}^{(2,2)*}$ the comparison is

$$\Omega_{CL}^{(2,2)*} = .67615$$

$$\frac{\partial \Omega^{(2,2)*}}{\partial \lambda} = -.02948 \qquad (6.2\text{-}12)$$

$$\frac{\partial^2 \Omega^{(2,2)*}}{\partial \lambda^2} = .00746$$

$$\text{Sum} = .65413 \qquad \Omega_{CL}^{(2,2)*}\Big|_{L-J} = .64924$$

As in the case of the $\Omega_{CL}^{(\ell)*}$ the agreement is very good. However, the agreement is not quite as good, as is expected from the comments above.

For $\Omega_{II}^{(1,1)*}$ the comparison at a reduced temperature of 50 is

$$\Omega_{II}^{(1,1)*} = 3.4608 \times 10^{-5}$$

$$\frac{\partial \Omega_{II}^{(1,1)*}}{\partial \lambda} = -7.9547 \times 10^{-5} \qquad (6.2\text{-}13)$$

$$\text{Sum} = -4.4939 \times 10^{-5} \qquad \Omega_{II}^{(1,1)*}\Big|_{L-J} = -1.9272 \times 10^{-4}$$

For $\Omega_{II}^{(2,2)*}$ the comparison is

$$\Omega_{II}^{(2,2)*} = 2.6076 \times 10^{-4} \qquad (6.2\text{-}14)$$

$$\frac{\partial \Omega_{II}^{(2,2)*}}{\partial \lambda} = -.9351 \times 10^{-4}$$

$$\text{Sum} = 1.6725 \times 10^{-4} \quad \Omega_{II}^{(2,2)*}\Big|_{L-J} = 1.2231 \times 10^{-4}$$

These results emphasize the remarks above concerning the behavior of the $\Omega^{(\ell,s)*}$ in relation to the transform nature of these integrals. The agreement for $\Omega_{II}^{(2,2)*}$ is fair, but not quite as good as $Q_{II}^{(2)*}$; the agreement for $\Omega_{II}^{(1,1)*}$ is poor, even poorer than for $Q_{II}^{(1)*}$.

For $\Omega_{IV}^{(1,1)*}$ the comparison at this reduced temperature is

$$\Omega_{IV}^{(1,1)*} = 1.6841 \times 10^{-6} \quad \Omega_{IV}^{(1,1)*}\Big|_{L-J} = 6.0885 \times 10^{4} \qquad (6.2\text{-}15)$$

For $\Omega_{IV}^{(2,2)*}$ the comparison is

$$\Omega_{IV}^{(2,2)*} = 1.3649 \times 10^{-6} \quad \Omega_{IV}^{(2,2)*}\Big|_{L-J} = 3.1129 \times 10^{1} \qquad (6.2\text{-}16)$$

The agreement here is extremely poor, especially for $\Omega_{IV}^{(1,1)*}$

The reason for this is again the nature of the omega integrals; they have contributions from all energies. The $Q_{IV}^{(l)*}$ become extremely large at low reduced energies and weight the $\Omega_{IV}^{(l,s)*}$ heavily even at a reduced temperature of 50 (the behavior of the $Q^{(l)*}$ for the Lennard-Jones potential is discussed in the next sections).

In general, the comparisons are quite good. This creates confidence in both the perturbation calculations and the calculations for the Lennard-Jones potential. Not only do the high reduced energy $Q^{(l)*}$ check but the high reduced temperature behavior of the $\Omega^{(l,s)*}$ is as expected, which serves somewhat as a check on the $Q^{(l)*}$ of lower reduced energy.

The crossover of $Q_{qu}^{(2)*}$ and $Q_{CL}^{(2)*}$ which is touched upon in the introduction to Chapter IV is discussed in the next section.

3. The Lennard-Jones (12-6) Potential

The existence of a minimum in the potential function has a very marked effect on the low energy behavior of the $Q^{(l)*}$, which differs greatly from the low energy behavior for the monotonic potential. While the classical limits are effected least in magnitude, the inclusion of the inner region into the τ integration for reduced energies below .8 is probably the most profound result of these calculations. The effects on the classical limits of $Q^{(1)*}$ and $Q^{(2)*}$ are markedly different. In the three turning point region

the classical limit of $Q^{(1)*}$ is always greater than the classical value. For $Q^{(2)*}$ the situation is not so straightforward. For a reduced energy of .8 down to about .3 the classical limit is slightly less than the classical value. Below a reduced energy of about .3 , however, the classical limit is greater than the classical value. It may be possible to explain this increase in $Q_{CL}^{(1)*}$ and decrease in $Q_{CL}^{(2)*}$ by examining the integrals for the classical limits. The classical limits of Eqns. (2.2-17) and (2.2-18) may be written

$$Q_{CL}^{(1)*} = 2\int_0^\infty (1 - \cos\chi_{20})\, b\, d\, b$$

$$Q_{CL}^{(2)*} = 3\int_0^\infty (1 - \cos^2\chi_{20})\, b\, d\, b \qquad (6.3\text{-}1)$$

Since in $Q_{CL}^{(2)*}$ the integrand involves $\cos^2\chi_{20}$, the integrand is always less than or equal to b . However, in $Q_{CL}^{(1)*}$ the integrand involves just $\cos 2\chi_{20}$ and thus can be as great as $2b$ It may be, then, that the inner region contributes just enough to χ_{20} to alter the integrands so as to reduce $Q_{CL}^{(2)*}$ and increase $Q_{CL}^{(1)*}$ in the range of energies from .3 to .8 . Plots of the classical and classical limits of $Q^{(1)*}$ and $Q^{(2)*}$ are shown in Figs. (6.3-1) and (6.3-2).

Since the classical limits of the $Q^{(l)*}$ are different from the classical values below a reduced energy of .8, the classical limits of the $\Omega^{(l,s)*}$ differ from the classical values over an extended range of temperature. The classical limit of $\Omega^{(1,1)*}$

is greater than the classical value up to a reduced temperature of about 5 . At a reduced temperature of .2 the classical limit is about 20 per cent larger than the classical value. This difference decreases rapidly and is only about 4 per cent at a reduced temperature of .5.

One aspect of this increase in the classical limit over the classical value of $\Omega^{(1,1)*}$ is particularly interesting. In a quantum mechanical calculation of the omega integrals, Imam-Rahajoe, Curtiss, and Bernstein[12] found that for reduced temperatures between .3 and 5 the $\Omega^{(1,1)*}$ calculated for $\Lambda^* = 3$ was less than $\Omega^{(1,1)*}$ calculated for $\Lambda^* = 2$ which was less than $\Omega^{(1,1)*}$ calculated for $\Lambda^* = 1$. For reduced temperatures greater than .6 , the classical values of $\Omega^{(1,1)*}$ as calculated by Monchick and Mason[33] are greater than the $\Omega^{(1,1)*}$ calculated for $\Lambda^* = 1$. However, for reduced temperatures between .3 and .6 the classical values are <u>less</u> than the $\Omega^{(1,1)*}$ calculated for $\Lambda^* = 1$. But the classical limit as calculated in this thesis is greater than $\Omega^{(1,1)*}$ for $\Lambda^* = 1$ over the entire range of reduced temperatures down to .1 . Below a reduced temperature of about .1 the $\Omega^{(1,1)*}$ for the various values of Λ^* cross one another and the order is not that described above.

The classical limit of $\Omega^{(2,2)*}$ is practically equal to the classical value of $\Omega^{(2,2)*}$. Above a reduced temperature of .2 the classical limit is slightly greater; below .2 it is considerably greater than the

classical value. Unfortunately, while the classical limit of $\Omega^{(2,2)*}$ is greater than the classical value, it is not large enough to be greater than $\Omega^{(2,2)*}$ for $\Lambda^* = 1$ for reduced temperatures below about .4 .

The general nature of the quantum corrections to the $Q^{(\ell)*}$ is that they are quite large for reduced energies below .8 (in the three turning point region) and well behaved and small for reduced energies above .8 . That this is the case is not too surprising because it was suspected from the beginning that the series was asymptotic.

The quantum corrections to the omega integrals, as would be expected, are small at high reduced temperatures and large at low reduced temperatures. The terms in Λ^{*4} are exceptions to this and are somewhat disappointing in that they are large even at reduced temperatures of 50 .

A comparison of the quantum corrections for $\Omega^{(\ell,s)*}$ with previously published[11,12] quantum mechanical results for fixed values of Λ^* is difficult because of the magnitude of quantum corrections. The terms linear and cubic in Λ^{*3} are negligibly small except at low values of the reduced temperature where all of the other quantum corrections are even larger. The terms quadratic in Λ^* are the most interesting of the quantum corrections. Both $\Omega_{II}^{(1,1)*}$ and $\Omega_{II}^{(2,2)*}$ reflect nicely the behavior of their respective $Q_{II}^{(\ell)*}$. However, both are so

small at high reduced temperatures in comparison to their respective classical limits, that except for large Λ^* (e.g., about $\Lambda^* = 4$, which is unrealistic for large reduced temperatures) they are of the same magnitude as the numerical uncertainty in the classical limits. Even so, as was shown by the perturbation calculations in the last section, these values of $\Omega_{II}^{(\ell,s)*}$ and $Q_{II}^{(\ell)*}$ are probably correct.

If the magnitude of the $\Omega_{II}^{(\ell,s)*}$ is such that the results cannot be checked at high reduced temperatures, their signs offer further confirmation that they are correct. The quantum calculation[11,12] of $\Omega^{(1,1)*}$ and $\Omega^{(2,2)*}$ show that for reduced temperature of about 50 $\Omega_{qu}^{(1,1)*}$ is less than, and $\Omega_{qu}^{(2,2)*}$ greater than the corresponding classical values. The signs of $\Omega_{II}^{(1,1)*}$ and $\Omega_{II}^{(2,2)*}$ at a reduced temperature of 50 confirm this.

At lower values of the reduced temperature the effect of the very large $Q_{II}^{(\ell)*}$ and $Q_{IV}^{(\ell)*}$ for reduced energies below .8 weights the quantum corrections $\Omega_{II}^{(\ell,s)*}$ and $\Omega_{IV}^{(\ell,s)*}$ to a very great extent. This is particularly noticeable in $\Omega_{II}^{(2,2)*}$ which is positive for reduced temperatures less than 13 instead of becoming increasingly negative at lower values of the reduced temperature as the quantum calculations indicate it should. On the other hand, $\Omega_{II}^{(1,1)*}$ is too negative at the low reduced temperature end. Below a reduced temperature of about 2 the

quantum corrections become very large.

The high reduced temperature behavior of the $\Omega^{(l,s)*}$ is very much the same as the high reduced energy behavior of the $Q^{(l)*}$. It is apparent that $Q_{II}^{(2)*}$ goes from negative to positive, passes through a maximum and decreases slowly with increasing reduced energy. The same phenomenon would be observed in $\Omega_{II}^{(2,2)*}$ if the reduced temperature range was extended further. The crossover from negative to positive is the one originally proposed by de Boer and Bird.[13] Since the quantum corrections $Q_{II}^{(2)*}$ and $Q_{IV}^{(2)*}$ at high reduced energy are both positive such a crossover of the classical and quantum curves does occur. The actual point on the reduced energy scale where the crossover does occur is a function of Λ^*. However, for reasonable Λ^* the crossover occurs at an energy so high that the quantum corrections are about nil compared to the classical limit.

On the following pages are presented various graphs and tables associated with the quantities calculated in this thesis.